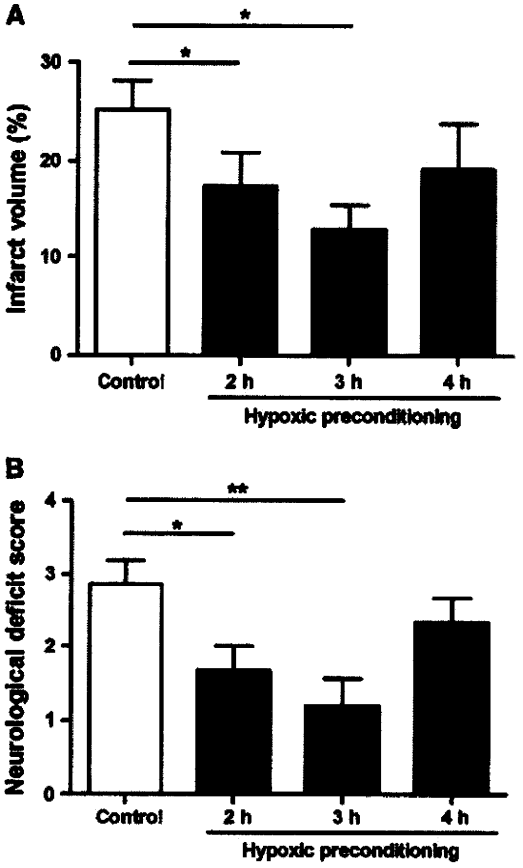

Figure 1 Effect of hypoxic preconditioning (8% O_2) on infarct volume and neurologic scores after transient MCAO in wild-type mice. Mice were exposed to hypoxia for 2, 3, or 4 hours. Forty-eight hours later, MCAO was induced for 30 minutes. (**A**) Infarct volume and (**B**) neurologic scores were determined 24 hours after the insult. Infarct volume was expressed as the percentage of the infarcted tissue in reference to the contralateral hemisphere. Values show mean ± s.e.m. $n = 10$ to 15 for each group; $^*P < 0.05$ and $^{**}P < 0.01$. MCAO, middle cerebral artery occlusion.

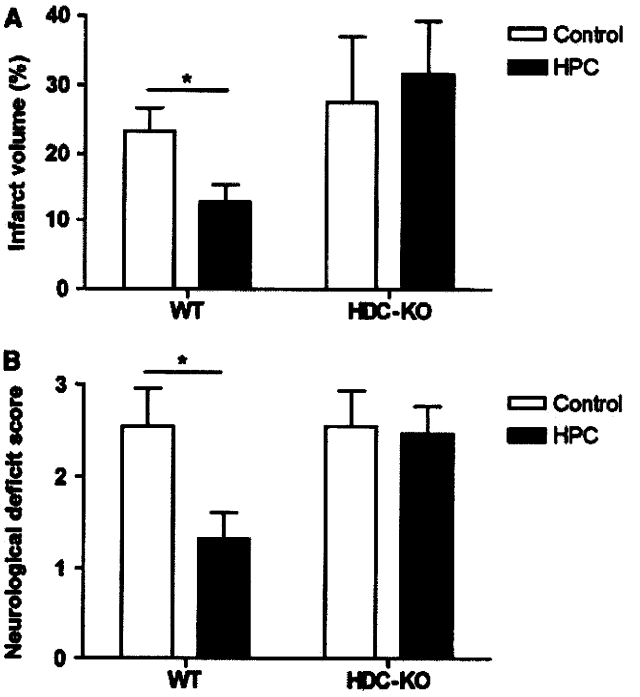

Figure 2 Effect of hypoxic preconditioning (HPC; 8% O_2) on transient MCAO-induced injury in wild-type (WT) and histidine decarboxylase knockout (HDC-KO) mice. Forty-eight hours after 3 hours of hypoxic preconditioning or normoxia, MCAO was induced for 30 minutes. (**A**) Infarct volume and (**B**) neurologic scores were determined 24 hours after MCAO in WT and HDC-KO mice. Values show mean ± s.e.m. $n = 8$ to 12 for each group; $^*P < 0.05$. MCAO, middle cerebral artery occlusion.

ditioned animals was paralleled by functional changes in neurologic deficits. Animals preconditioned for 2 or 3 hours exhibited lower neurologic deficit scores at 24 hours after transient MCAO ($P < 0.05$) relative to control animals (Figure 1B).

To determine whether histamine is involved in hypoxic preconditioning, we used HDC-KO mice, which lack the synthetic enzyme for histamine. Three hours of hypoxic preconditioning induced the strongest neuroprotection; therefore, we compared the effects of 3 hours of preconditioning on WT and HDC-KO mice. No significant differences in infarct volume and neurologic deficit scores were found between the control groups of WT and HDC-KO mice 24 hours after 30 minutes of MCAO (Figure 2). In HDC-KO mice, hypoxic preconditioning did not decrease the infarct volume or improve neurologic function compared with the nonpreconditioned group. Similarly, the histamine synthesis enzyme inhibitor α-FMH reversed the neuroprotection induced by hypoxic preconditioning in infarct volume and neurologic scores in WT mice ($P < 0.05$; Figures 3A and 3B), whereas α-FMH alone had no effect on infarct volume without hypoxic preconditioning (infarct volume: control group, 23.63% ± 3.72%, $n = 4$; α-FMH-treated group, 22.72% ± 5.15%, $n = 5$). In contrast, hypoxic preconditioning combined with histamine (5 μg/2 μL per 6 h per animal for 3 injections, intracerebroventricularly) in HDC-KO mice significantly improved neurologic function and decreased infarct volume ($P < 0.05$; Figures 3C and 3D), whereas histamine alone had no effect on infarct volumes without hypoxic preconditioning (infarct volume: vehicle group, 26.59% ± 4.36%, $n = 4$; histamine-treated group, 23.44% ± 2.60%, $n = 6$). In addition, mean arterial blood pressure, heart rate, and arterial blood gas (pH, PaO_2, $PaCO_2$) before and after ischemia did not differ among the six groups (Supplementary Table 2).

Hypoxic Preconditioning Ameliorated the Reduction in the Peripheral Cerebral Blood Flow During Transient Focal Cerebral Ischemia in Wild-Type Mice but not in Histidine Decarboxylase Knockout Mice

Cerebral blood flow was measured in the core and peripheral regions of the MCA territory. As shown in

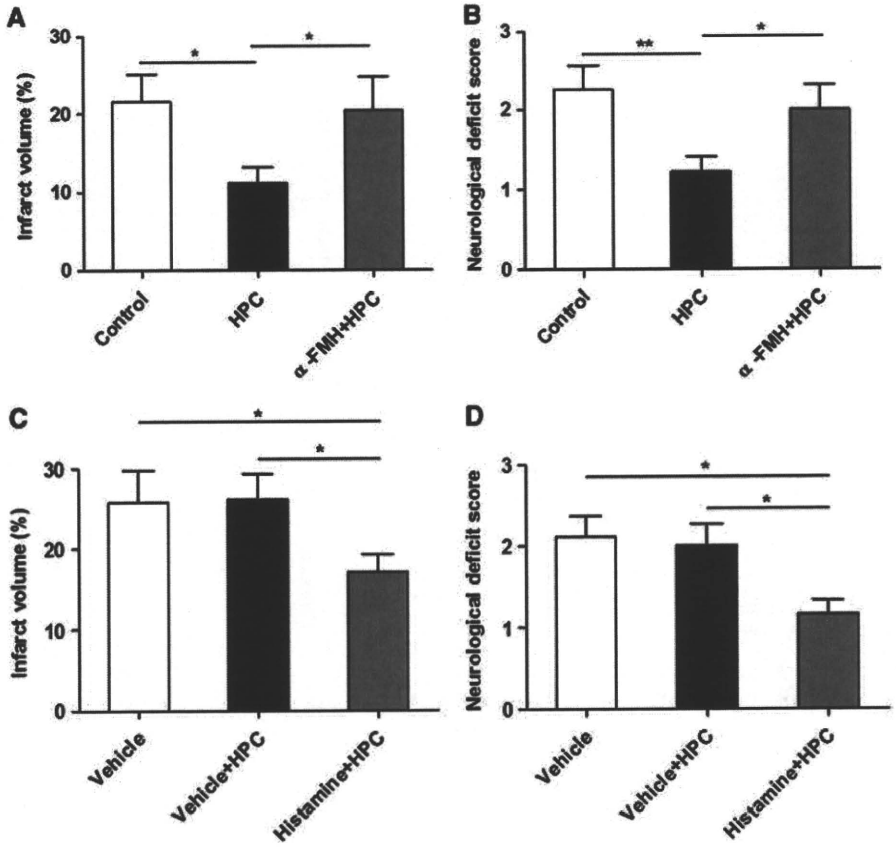

Figure 3 Effect of hypoxic preconditioning (HPC; 8% O_2) on transient MCAO-induced injury in α-FMH-treated wild-type (WT) mice and histamine-treated histidine decarboxylase knockout (HDC-KO) mice. Forty-eight hours after 3 hours of hypoxic preconditioning or normoxia, MCAO was induced for 30 minutes. α-FMH (25 mg/kg) was injected intraperitoneally 3 hours before hypoxic preconditioning in WT mice, and (**A**) infarct volume and (**B**) neurologic scores were determined 24 hours after MCAO. Histamine (5 μg/2 μL per 6 h per animal for 3 injections; the first injection was administered 30 minutes before hypoxia.) was administered intracerebroventricularly with hypoxic preconditioning in HDC-KO mice, and (**C**) infarct volume and (**D**) neurologic scores were determined 24 hours after MCAO. Values show mean ± s.e.m. $n = 8$ to 12 for each group; $^*P < 0.05$ and $^{**}P < 0.01$. α-FMH, α-fluoromethylhistidine; MCAO, middle cerebral artery occlusion.

Figure 4A, no difference in CBF changes of the core region was detected among the five groups during and after MCAO. However, 33.7% increased blood flow was observed in the peripheral region during ischemia in the hypoxic preconditioned group of WT mice. In contrast, in HDC-KO and α-FMH-treated WT mice, hypoxic preconditioning aggravated the reduction in peripheral CBF by 42.5 and 40.5% of the control groups, respectively (Figure 4B).

Effect of Hypoxia on Histamine Content and Histidine Decarboxylase Activity in the Cerebral Cortex of Wild-Type Mice

After hypoxia, the cortex of WT mice was isolated for HPLC determination of histamine concentration and HDC activity. The histamine levels after 2, 3, and 4 hours of hypoxia were 69.3, 65.5, and 66.6% (all $P < 0.05$) of the control group, respectively (Figure 5A). Histidine decarboxylase activity in the control group was 156.00 ± 21.51 fmol/min per mg protein. Three hours of hypoxia significantly increased HDC activity (236.1 ± 14.68 fmol/min per mg protein, $P < 0.0.5$, Figure 5B). In addition, HDC mRNA of the hypothalamus where histamine-producing neurons are located after 3 hours of hypoxia was not significantly changed compared with the control group (Figure 5C).

Vascular Endothelial Growth Factor is Induced by Hypoxic Preconditioning in Wild-Type but Not in Histidine Decarboxylase Knockout Mice

Both WT and HDC-KO mice were exposed to 8% O_2 for 3 hours. After various times of reoxygenation in normal air, the cerebral cortex was collected for analysis of VEGF mRNA and protein. Real-time PCR analysis showed upregulated expression of VEGF mRNA (including VEGF165, VEGF121, and VEGF140 isoforms) after 3 hours of hypoxia ($P < 0.05$), which then rapidly decreased to baseline after 3 hours of reoxygenation in both WT and HDC-KO mice (Figure 6A). However, the VEGF mRNA level in WT mice (6.59 ± 1.46-fold control WT,

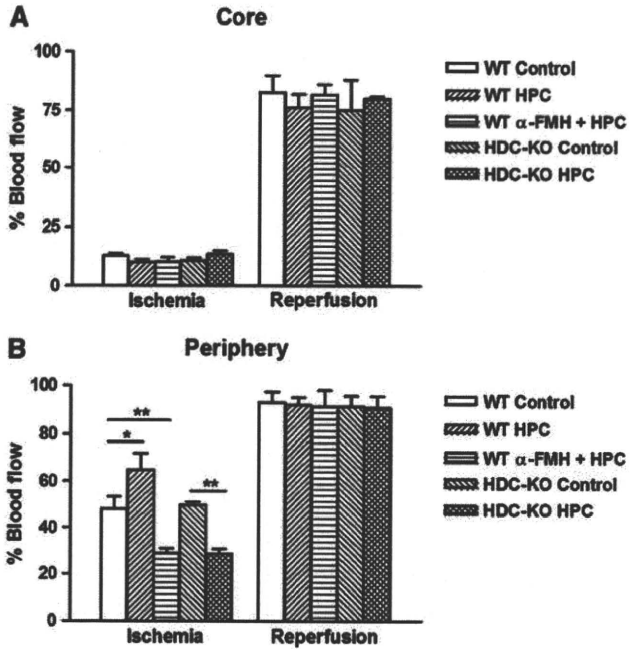

Figure 4 Effect of hypoxic preconditioning (HPC; 3 hours, 8% O_2) on cerebral blood flow (CBF) during transient MCAO in wild-type (WT) mice treated with or without α-FMH and histidine decarboxylase knockout (HDC-KO) mice. α-FMH (25 mg/kg) was injected intraperitoneally 3 hours before hypoxic preconditioning. CBF was measured in (**A**) the core and (**B**) the periphery of the MCA territory before, during, and after MCAO. CBF was expressed as a percentage of the value before MCAO. Values show mean ± s.e.m. (Panel **A**) $n = 8$ to 12 for each group; (panel **B**) $n = 8$ to 9 for each group; $^*P < 0.05$, $^{**}P < 0.01$. α-FMH, α-fluoromethylhistidine; MCAO, middle cerebral artery occlusion.

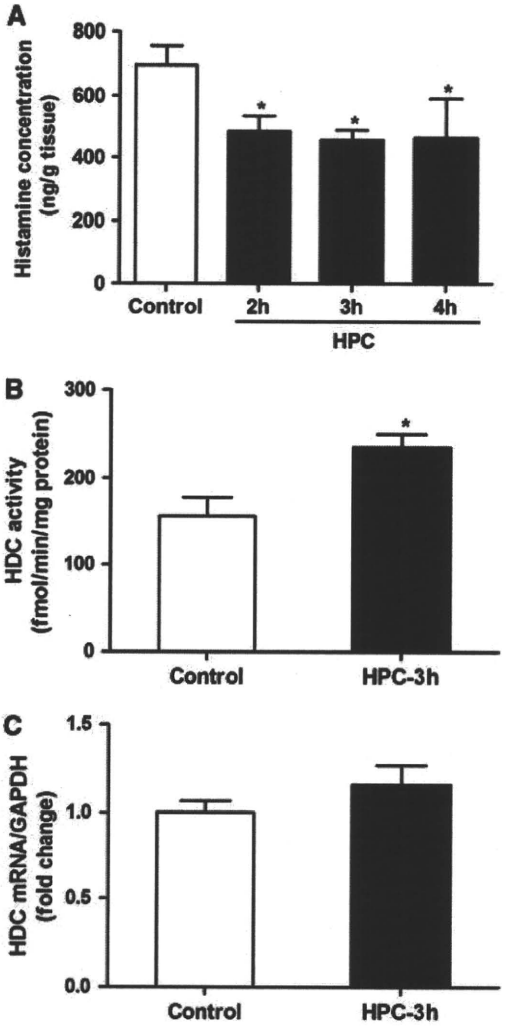

Figure 5 Effect of hypoxic preconditioning (HPC, 8% O_2) on histamine levels and histidine decarboxylase (HDC) activity of the cortex and HDC mRNA expression of the hypothalamus in wild-type mice. (**A**) Histamine levels in the cortex were assayed at 2, 3, and 4 hours of hypoxia. (**B**) HDC activity in the cortex and (**C**) HDC mRNA expression of the hypothalamus were assayed at 3 hours of hypoxia. Values show mean ± s.e.m. $n = 4$ to 6 for each group; $^*P < 0.05$ versus control group.

$P < 0.05$) was higher than that in HDC-KO mice (3.08 ± 0.77-fold control WT, $P < 0.05$) immediately after hypoxia ($P < 0.05$). Otherwise, the cortex of both WT and HDC-KO mice not exposed to hypoxia showed similar levels of VEGF mRNA, indicating that histamine is not required for the constitutive expression of VEGF in the cortex under normal physiologic conditions. Similarly, VEGF protein expression (VEGF165 isoform) in WT mice increased at as early as 3 hours of hypoxia ($P < 0.01$), remained upregulated after 8 hours of reoxygenation ($P < 0.01$), and then normalized after 24 hours of reoxygenation. Interestingly, in HDC-KO- and α-FMH-treated WT mice, no significant increase in the VEGF protein occurred at various times of reoxygenation (Figures 6C and 6D). In addition, erythropoietin, which has also been found to be a key mediator in hypoxic preconditioning, responded similarly in both HDC-KO and WT mice (Figure 6B).

Effect of VEGFR2 Antagonist SU1498 on Neuroprotection Induced by Hypoxic Preconditioning

The VEGFR2 antagonist SU1498 or vehicle was administered intracerebroventricularly 30 minutes before hypoxic preconditioning, followed by two infusions (with an interval of 12 hours). SU1498 prevented the protective effect of hypoxic preconditioning in infarct volume in WT mice having transient focal cerebral ischemia ($P < 0.05$; Figure 7A). It reversed the improved peripheral CBF induced by hypoxic preconditioning ($P < 0.05$; Figure 7B). In addition, SU1498 alone had no effect on infarct volume in the absence of hypoxic preconditioning (infarct volume: vehicle group, 26.02% ± 6.18%, $n = 4$; SU1498-treated group, 26.55% ± 5.55%, $n = 5$).

Discussion

In this study, we showed for the first time that histamine is involved in hypoxia-induced ischemia

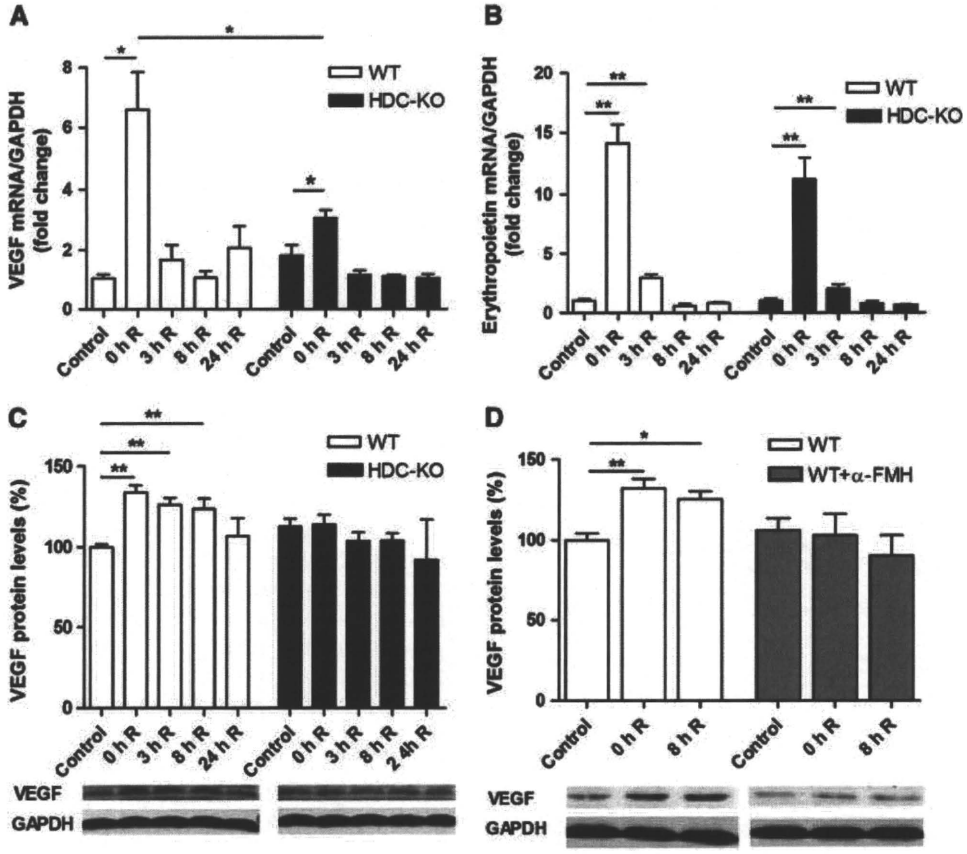

Figure 6 Effect of hypoxic preconditioning (3 hours, 8% O_2) on expression of VEGF mRNA and protein in wild-type (WT) and histidine decarboxylase knockout (HDC-KO) mice. (**A**) VEGF mRNA expression, (**B**) erythropoietin mRNA expression, and (**C**) VEGF protein expression in the cerebral cortex of WT and HDC-KO mice at 0, 3, 8, and 24 hours after reoxygenation. (**D**) VEGF protein expression in the cerebral cortex of WT mice treated with or without α-FMH (25 mg/kg, intraperitoneally) at 0 and 8 hours after reoxygenation. Values show mean ± s.e.m. $n = 5$ to 6 for each group; $^*P < 0.05$ and $^{**}P < 0.01$. α-FMH, α-fluoromethylhistidine; R, reoxygenation; VEGF, vascular endothelial growth factor.

tolerance in the adult brain. Three hours of hypoxic preconditioning performed 48 hours before transient MCAO afforded a significantly better outcome in WT mice, as shown by remarkable reductions in infarct volume and neurologic deficit. This result is in agreement with Miller *et al* (2001), and in their experiment, animals were exposed to 2 hours of hypoxia (11% O_2) 48 hours before transient MCAO. However, in HDC-KO mice which chronically lack histamine, the protection induced by hypoxic preconditioning completely disappeared, and hypoxic preconditioning combined with histamine produced neuroprotection in HDC-KO mice. The infused histamine exerted in the central nervous system but not in the peripheral system, because histamine cannot cross the blood–brain barrier and 3 hours of hypoxic preconditioning combined with histamine treatment did not obviously influence the permeability of the blood–brain barrier in HDC-KO mice (data not shown). Alpha-FMH is a specific and irreversible inhibitor of HDC, and a single administration decreases the histamine content in the neuronal pool only, without affecting nonneuronal sources in the brain (Garbarg *et al*, 1980). Indeed, α-FMH also clearly reversed the neuroprotection induced by hypoxic preconditioning in our experiments. These data show that endogenous histamine is an important mediator in hypoxia-induced tolerance to stroke in adult mice. Furthermore, we found that histamine content significantly decreased in the cortex of WT mice at 2, 3, and 4 hours of hypoxia, and that HDC activity increased at 3 hours of hypoxia, which indicates that hypoxia increased the release of histamine in the mouse cortex (It must be noted that as extracellular histamine is rapidly degraded, massive release results in the depletion of intracellular histamine.) Taken together, our results support the hypothesis that an increase in histamine release resulting from activation of histaminergic neurons is necessary for the induction of hypoxic preconditioning.

In our preconditioning paradigm, hypoxia (8% O_2) produced a bell-shaped curve for protection against a transient MCAO, having a peak at 3 hours. A longer period of hypoxia (4 hours) did not result in significant protection, although this did induce a release of histamine comparable with hypoxia for 2 or 3 hours. Prass *et al* (2003) reported similar

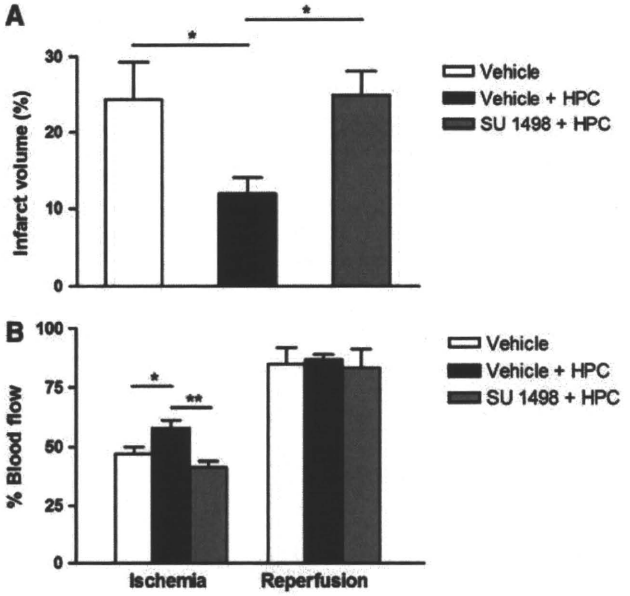

Figure 7 Effect of hypoxic preconditioning (HPC; 8% O_2) on transient MCAO-induced injury in wild-type mice treated with VEGFR2/Flk1 antagonist SU1498. Forty-eight hours after 3 hours of hypoxic preconditioning or normoxia, MCAO was induced for 30 minutes. (**A**) SU1498 (250 ng/2 μL per 12 h per animal for 3 injections; the first injection was administered 30 minutes before hypoxia) was administered intracerebroventricularly with hypoxic preconditioning in wild-type mice, and the infarct volume was determined 24 hours after MCAO. (**B**) CBF was measured in the peripheral region of the MCA territory before, during and after MCAO. CBF was expressed as a percentage of the value before MCAO. Values show mean ± s.e.m. $n = 5$ to 8 for each group; $^*P < 0.05$, $^{**}P < 0.01$. CBF, cerebral blood flow; MCAO, middle cerebral artery occlusion; VEGFR, vascular endothelial growth factor receptor.

results which showed a peak at 5 hours, whereas a longer period (6 hours) induced severe damage in the CA1 region. It is still unknown why the protection disappears with time. This is not likely to be related to the glutamate excitotoxicity induced by hypoxia, because the glutamate content after 4 hours of hypoxia was not significantly changed from that of the control group (data not shown), and glutamate in synaptic terminals is not reduced by hypoxia in rat hippocampal slices (Madl and Royer, 1999). Other factors, such as hypotension (Prass *et al*, 2003) and hypocapnia induced by hypoxia may be of relevance, because hypocapnia with hypotension causes hippocampal neuronal death (Ohyu *et al*, 2000), and hypocapnia activates caspase-3 to induce apoptosis (Xie *et al*, 2004). The narrow effective range for the duration of hypoxic preconditioning greatly restricts its direct clinical application. Therefore, aiming at effective targets in the protection process will be more productive. In our system, the release of histamine maintains a stable level during hypoxia, and histamine is a known neuroprotective factor. Thus, regulating histaminergic neuronal activity to maintain a specific level of histamine may be more controllable and safer against stroke, without the side effects of overlong hypoxia.

In the search for mechanisms involved in the effect of histamine on hypoxic preconditioning, we found that hypoxia-induced VEGF mRNA expression was higher in the cerebral cortex of WT mice than HDC-KO mice, and that VEGF165 protein expression was induced by hypoxia in WT mice but not in HDC-KO or α-FMH-treated WT mice, which strongly indicates that the lack of histamine can inhibit VEGF expression induced by hypoxia. Vascular endothelial growth factor protects the brain against ischemia and is involved in the establishment of hypoxic preconditioning (Bernaudin *et al*, 2002; Laudenbach *et al*, 2007; Wick *et al*, 2002). Bernaudin *et al* (2002) reported that hypoxia induces tolerance to cerebral ischemia in association with increased expression of VEGF in the adult mouse brain. Neuroprotection induced by hypoxic exposure is diminished by administration of the anti-VEGFR2/Flk1 blocking antibody or by the use of mutant mice lacking the hormone response element of the VEGF gene promoter in newborn mice (Laudenbach *et al*, 2007). Histamine enhances VEGF production in the granulation tissue and in cyclooxygenase-2-positive HT29 and Caco-2 cells through the H_2 receptor (Cianchi *et al*, 2005; Ghosh *et al*, 2001, 2002). We also found that endogenous histamine induced the expression of VEGF mRNA and protein in the cerebral cortex on exposure to hypoxia. Furthermore, SU1498, a VEGFR2/Flk1 antagonist, inhibited the neuroprotection induced by hypoxic preconditioning in WT mice. As histamine is proved to be involved in hypoxic preconditioning-induced neuroprotection in this study, it is likely that the robust neuroprotection is established by VEGF production induced by histamine release.

In WT mice, the expression of hypoxia-inducible factor-1α, which is a main transcription factor involved in the induction of VEGF (Bernaudin *et al*, 2002), was higher than that in HDC-KO mice immediately after hypoxia, and α-FMH also inhibited hypoxia-inducible factor-1α production induced by hypoxia (Supplementary Figure 1). Hypoxia (O_2 tension < 0.2%) can increase HDC mRNA expression by induction of hypoxia-inducible factor-1α (Jeong *et al*, 2009). However, in our present system, HDC mRNA level of the hypothalamus, where histamine-producing neurons are located, was not significantly changed after hypoxia. This conflict may be attributed to different hypoxic conditions, because O_2 tension < 0.2% is much severer than 8% O_2. These results at least imply that histamine mediated VEGF expression in hypoxia likely through regulating hypoxia-inducible factor-1α expression. In addition, erythropoietin has also been found to be a key mediator in hypoxic preconditioning (Prass *et al*, 2003). In this study, in HDC-KO mice, erythropoietin response was similar to that measured in WT mice. It suggests that erythropoietin may be not involved in histamine induced-protection in hypoxic preconditioning. As the exogenous

treatment of recombinant human erythropoietin increases brain levels of VEGF after stroke (Wang *et al*, 2004), erythropoietin may also be involved in hypoxic preconditioning-induced VEGF production beside histamine.

Vascular endothelial growth factor itself has a direct neuroprotective effect on neurons. Vascular endothelial growth factor protects cultured hippocampal neurons and several neuronal cell lines against cell death induced by ischemia or excitotoxic stimuli through the VEGFR2/phosphoinositide 3-kinase/Akt and VEGFR2/MEK/ERK signaling pathways (Jin *et al*, 2000; Matsuzaki *et al*, 2001; Qiu *et al*, 2003). In cultured cerebellar granule neurons, hypoxia-induced tolerance also depends on VEGF/VEGFR2 activation and Akt phosphorylation (Wick *et al*, 2002). However, once the dose of VEGF exceeds the limit, adverse effects of VEGF might surpass the neuroprotective effects and deteriorate neuronal survival and function *in vivo* and *in vitro* (Laudenbach *et al*, 2007; Manoonkitiwongsa *et al*, 2004; Yasuhara *et al*, 2005). Interestingly, we also found that 3 hours of hypoxia (8% O_2) induced a moderate upregulation (34%) of the VEGF protein in WT mice. These results indicate the importance of maintaining VEGF levels in a suitable range for neuroprotection against ischemia, and that low levels of VEGF expression in response to mild hypoxia may be necessary for neuroprotection. A moderate regulator of VEGF such as histamine may be safer for the treatment of stroke.

In addition, an increase in CBF is considered to contribute to protection against brain ischemia. Our previous study has shown that histamine elicits an increase in CBF in the rat hippocampus through both the postsynaptic H1, H2 receptors and the presynaptic H3 receptor (Chen, 2001; Suzuki *et al*, 1999). Therefore, we measured CBF in the core and peripheral regions of the MCA territory. Although CBF in the core region showed no significant difference among the groups, hypoxic preconditioning elevated CBF in the peripheral region of WT mice. In HDC-KO mice or WT mice treated with α-FMH, hypoxic preconditioning aggravated the reduced CBF in the peripheral region during ischemia compared with nonpreconditioned animals, whereas histamine administered in HDC-KO mice reversed the decreased peripheral CBF after hypoxic preconditioning (data not shown). These data suggest that histamine mediates the enhanced CBF produced by hypoxia preconditioning. Besides the direct vasodilation effect of histamine, VEGF may be another mechanism conferring increased CBF. Vascular endothelial growth factor is a regulator of CBF by inducing nitric oxide production or enhancing angiogenesis (Vogel *et al*, 2003; Zhang *et al*, 2000). It was interesting to find that SU1498 reversed the increased peripheral CBF induced by hypoxic preconditioning in WT mice, and histamine elevated VEGF expression in this study or in other reports (Ghosh *et al*, 2001, 2002), suggesting that histamine release induced by hypoxic preconditioning might also improve peripheral CBF in ischemia partly through the VEGF/VEGFR2/Flk1 pathway.

In conclusion, this study indicates that endogenous histamine has an essential role in hypoxia-induced ischemic tolerance in brain. The beneficial effects of histamine in hypoxic preconditioning may occur through upregulating VEGF expression. Further studies will need to be conducted to understand the mechanisms of action of histamine in hypoxic preconditioning that lead to protection of the brain against ischemia and neurodegenerative disorders.

Acknowledgments

We are very grateful to Dr Iain C. Bruce for reading the manuscript.

Disclosure/conflict of interest

The authors declare no conflict of interest.

References

Adachi N (2005) Cerebral ischemia and brain histamine. *Brain Res Brain Res Rev* 50:275–86

Bernaudin M, Nedelec AS, Divoux D, MacKenzie ET, Petit E, Schumann-Bard P (2002) Normobaric hypoxia induces tolerance to focal permanent cerebral ischemia in association with an increased expression of hypoxia-inducible factor-1 and its target genes, erythropoietin and VEGF, in the adult mouse brain. *J Cereb Blood Flow Metab* 22:393–403

Chen Z (2001) Effect of clobenpropit on regional cerebral blood flow in rat hippocampus. *Acta Pharmacol Sin* 22:355–60

Cianchi F, Cortesini C, Schiavone N, Perna F, Magnelli L, Fanti E, Bani D, Messerini L, Fabbroni V, Perigli G, Capaccioli S, Masini E (2005) The role of cyclooxygenase-2 in mediating the effects of histamine on cell proliferation and vascular endothelial growth factor production in colorectal cancer. *Clin Cancer Res* 11:6807–15

Dai H, Zhang Z, Zhu Y, Shen Y, Hu W, Huang Y, Luo J, Timmerman H, Leurs R, Chen Z (2006) Histamine protects against NMDA-induced necrosis in cultured cortical neurons through H receptor/cyclic AMP/protein kinase A and H receptor/GABA release pathways. *J Neurochem* 96:1390–400

Diaz-Trelles R, Novelli A, Vega JA, Marini A, Fernandez-Sanchez MT (2000) Antihistamine terfenadine potentiates NMDA receptor-mediated calcium influx, oxygen radical formation, and neuronal death. *Brain Res* 880:17–27

Dirnagl U, Simon RP, Hallenbeck JM (2003) Ischemic tolerance and endogenous neuroprotection. *Trends Neurosci* 26:248–54

Garbarg M, Barbin G, Rodergas E, Schwartz JC (1980) Inhibition of histamine synthesis in brain by alpha-fluoromethylhistidine, a new irreversible inhibitor: *in vitro* and *in vivo* studies. *J Neurochem* 35:1045–52

Ghosh AK, Hirasawa N, Ohuchi K (2001) Enhancement by histamine of vascular endothelial growth factor

production in granulation tissue via H(2) receptors. *Br J Pharmacol* 134:1419–28

Ghosh AK, Hirasawa N, Ohtsu H, Watanabe T, Ohuchi K (2002) Defective angiogenesis in the inflammatory granulation tissue in histidine decarboxylase-deficient mice but not in mast cell-deficient mice. *J Exp Med* 195:973–82

Haas H, Panula P (2003) The role of histamine and the tuberomamillary nucleus in the nervous system. *Nat Rev Neurosci* 4:121–30

Hayashi T, Abe K, Itoyama Y (1998) Reduction of ischemic damage by application of vascular endothelial growth factor in rat brain after transient ischemia. *J Cereb Blood Flow Metab* 18:887–95

Inaba S, Iwai M, Tomono Y, Senba I, Furuno M, Kanno H, Okayama H, Mogi M, Higaki J, Horiuchi M (2009) Exaggeration of focal cerebral ischemia in transgenic mice carrying human renin and human angiotensinogen genes. *Stroke* 40:597–603

Irisawa Y, Adachi N, Liu K, Arai T, Nagaro T (2008) Alleviation of ischemia-induced brain edema by activation of the central histaminergic system in rats. *J Pharmacol Sci* 108:112–23

Iwanami J, Mogi M, Okamoto S, Gao XY, Li JM, Min LJ, Ide A, Tsukuda K, Iwai M, Horiuchi M (2007) Pretreatment with eplerenone reduces stroke volume in mouse middle cerebral artery occlusion model. *Eur J Pharmacol* 566:153–9

Jeong HJ, Moon PD, Kim SJ, Seo JU, Kang TH, Kim JJ, Kang IC, Um JY, Kim HM, Hong SH (2009) Activation of hypoxia-inducible factor-1 regulates human histidine decarboxylase expression. *Cell Mol Life Sci* 66:1309–19

Jin CL, Yang LX, Wu XH, Li Q, Ding MP, Fan YY, Zhang WP, Luo JH, Chen Z (2005) Effects of carnosine on amygdaloid-kindled seizures in Sprague-Dawley rats. *Neuroscience* 135:939–47

Jin KL, Mao XO, Greenberg DA (2000) Vascular endothelial growth factor: direct neuroprotective effect in *in vitro* ischemia. *Proc Natl Acad Sci USA* 97:10242–7

Laudenbach V, Fontaine RH, Medja F, Carmeliet P, Hicklin DJ, Gallego J, Leroux P, Marret S, Gressens P (2007) Neonatal hypoxic preconditioning involves vascular endothelial growth factor. *Neurobiol Dis* 26:243–52

Liu L, Zhang S, Zhu Y, Fu Q, Gong Y, Ohtsu H, Luo J, Wei E, Chen Z (2007) Improved learning and memory of contextual fear conditioning and hippocampal CA1 long-term potentiation in histidine decarboxylase knock-out mice. *Hippocampus* 17:634–41

Longa EZ, Weinstein PR, Carlson S, Cummins R (1989) Reversible middle cerebral artery occlusion without craniectomy in rats. *Stroke* 20:84–91

Madl JE, Royer SM (1999) Glutamate in synaptic terminals is reduced by lack of glucose but not hypoxia in rat hippocampal slices. *Neuroscience* 94:417–30

Manoonkitiwongsa PS, Schultz RL, McCreery DB, Whitter EF, Lyden PD (2004) Neuroprotection of ischemic brain by vascular endothelial growth factor is critically dependent on proper dosage and may be compromised by angiogenesis. *J Cereb Blood Flow Metab* 24:693–702

Matsuzaki H, Tamatani M, Yamaguchi A, Namikawa K, Kiyama H, Vitek MP, Mitsuda N, Tohyama M (2001) Vascular endothelial growth factor rescues hippocampal neurons from glutamate-induced toxicity: signal transduction cascades. *FASEB J* 15:1218–20

Miller BA, Perez RS, Shah AR, Gonzales ER, Park TS, Gidday JM (2001) Cerebral protection by hypoxic preconditioning in a murine model of focal ischemia-reperfusion. *Neuroreport* 12:1663–9

Ohyu J, Endo A, Itoh M, Takashima S (2000) Hypocapnia under hypotension induces apoptotic neuronal cell death in the hippocampus of newborn rabbits. *Pediatr Res* 48:24–9

Prass K, Scharff A, Ruscher K, Lowl D, Muselmann C, Victorov I, Kapinya K, Dirnagl U, Meisel A (2003) Hypoxia-induced stroke tolerance in the mouse is mediated by erythropoietin. *Stroke* 34:1981–6

Qiu MH, Zhang R, Sun FY (2003) Enhancement of ischemia-induced tyrosine phosphorylation of Kv1.2 by vascular endothelial growth factor via activation of phosphatidylinositol 3-kinase. *J Neurochem* 87:1509–17

Shen Y, Hu WW, Fan YY, Dai HB, Fu QL, Wei EQ, Luo JH, Chen Z (2007) Carnosine protects against NMDA-induced neurotoxicity in differentiated rat PC12 cells through carnosine-histidine-histamine pathway and H(1)/H(3) receptors. *Biochem Pharmacol* 73:709–17

Suzuki G, Chen Z, Sugimoto Y, Fujii Y, Kamei C (1999) Effects of histamine and related compounds on regional cerebral blood flow in rats. *Methods Find Exp Clin Pharmacol* 21:613–7

Vogel J, Horner C, Haller C, Kuschinsky W (2003) Heterologous expression of human VEGF165 in rat brain: dose-dependent, heterogeneous effects on CBF in relation to vascular density and cross-sectional area. *J Cereb Blood Flow Metab* 23:423–31

Wang L, Zhang Z, Wang Y, Zhang R, Chopp M (2004) Treatment of stroke with erythropoietin enhances neurogenesis and angiogenesis and improves neurological function in rats. *Stroke* 35:1732–7

Waskiewicz J, Molchanova L, Walajtys-Rode E, Rafalowska U (1988) Hypoxia and ischemia modifies histamine metabolism and transport in brain synaptosomes. *Resuscitation* 16:287–93

Wick A, Wick W, Waltenberger J, Weller M, Dichgans J, Schulz JB (2002) Neuroprotection by hypoxic preconditioning requires sequential activation of vascular endothelial growth factor receptor and Akt. *J Neurosci* 22:6401–7

Xie Z, Moir RD, Romano DM, Tesco G, Kovacs DM, Tanzi RE (2004) Hypocapnia induces caspase-3 activation and increases Abeta production. *Neurodegener Dis* 1:29–37

Yasuhara T, Shingo T, Muraoka K, wen Ji Y, Kameda M, Takeuchi A, Yano A, Nishio S, Matsui T, Miyoshi Y, Hamada H, Date I (2005) The differences between high and low-dose administration of VEGF to dopaminergic neurons of *in vitro* and *in vivo* Parkinson's disease model. *Brain Res* 1038:1–10

Yu GL, Wei EQ, Wang ML, Zhang WP, Zhang SH, Weng JQ, Chu LS, Fang SH, Zhou Y, Chen Z, Zhang Q, Zhang LH (2005) Pranlukast, a cysteinyl leukotriene receptor-1 antagonist, protects against chronic ischemic brain injury and inhibits the glial scar formation in mice. *Brain Res* 1053:116–25

Zhang ZG, Zhang L, Jiang Q, Zhang R, Davies K, Powers C, Bruggen N, Chopp M (2000) VEGF enhances angiogenesis and promotes blood-brain barrier leakage in the ischemic brain. *J Clin Invest* 106:829–38

Supplementary Information accompanies the paper on the Journal of Cerebral Blood Flow & Metabolism website (http://www.nature.com/jcbfm)

Free Radical Biology & Medicine 48 (2010) 727–735

Contents lists available at ScienceDirect

Free Radical Biology & Medicine

journal homepage: www.elsevier.com/locate/freeradbiomed

Original Contribution

Carnosine protects against permanent cerebral ischemia in histidine decarboxylase knockout mice by reducing glutamate excitotoxicity

Yao Shen [a,b,1], Ping He [b,1], Yan-ying Fan [b], Jian-xiang Zhang [b], Hai-jing Yan [b], Wei-wei Hu [b], Hiroshi Ohtsu [c], Zhong Chen [b,*]

[a] Institute of Molecular and Cellular Medicine, Wenzhou Medical College, Wenzhou 325035, China
[b] Institute of Neuroscience, Department of Pharmacology, College of Pharmaceutical Sciences, Zhejiang University, Hangzhou 310058, China
[c] Department of Engineering, Tohoku University School of Medicine, Aoba-ku, Sendai 980-8775, Japan

ARTICLE INFO

Article history:
Received 2 August 2009
Revised 14 December 2009
Accepted 22 December 2009
Available online 4 January 2010

Keywords:
Brain
Ischemia
Carnosine
Glutamate transporter-1
Mitochondrial function
Free radicals

ABSTRACT

Recently, we showed that carnosine protects against NMDA-induced excitotoxicity in differentiated PC12 cells through a histaminergic pathway. However, whether the protective effect of the carnosine metabolic pathway also occurs in ischemic brain is unknown. Utilizing the model of permanent middle cerebral artery occlusion (pMCAO) in mice, we found that carnosine significantly improved neurological function and decreased infarct size in both histidine decarboxylase knockout and the corresponding wild-type mice to the same extent. Carnosine decreased the glutamate levels and preserved the expression of glutamate transporter-1 (GLT-1) but not the glutamate/aspartate transporter in astrocytes exposed to ischemia in vivo and in vitro. It suppressed the dissipation of $\Delta\Psi_m$ and generation of mitochondrial reactive oxygen species (ROS) induced by oxygen–glucose deprivation in astrocytes. Furthermore, carnosine also decreased the mitochondrial ROS and reversed the decrease in GLT-1 induced by rotenone. These findings are the first to demonstrate that the mechanism of carnosine action in pMCAO may not be mediated by the histaminergic pathway, but by reducing glutamate excitotoxicity through the effective regulation of the expression of GLT-1 in astrocytes due to improved mitochondrial function. Thus, our study reveals a novel antiexcitotoxic agent in ischemic injury.

Ischemic stroke is the leading cause of neurological disability in adults and the second most common cause of death worldwide. Stroke is a complex insult, and glutamate excitotoxicity is one of the major underlying mechanisms [1,2]. Historically, research on stroke has mainly focused on neurons. However, multiple-target strategies for neuroprotection are emerging, and astrocytes, because of their diverse and significant roles, especially in glutamatergic signaling in stroke, have become a focus of attention [3].

Accumulating evidence demonstrates that histaminergic neurotransmission plays an important role in brain ischemia. Histamine or the H_2 receptor agonist, dimaprit, suppresses the neuronal degeneration after ischemia [4]. Inhibition of histamine signaling by α-fluoromethylhistidine (α-FMH) aggravates cerebral ischemic injury induced by 10 min of four-vessel occlusion in rats [5]. The H_3 receptor antagonist clobenpropit protects against NMDA-induced necrosis in cultured cortical neurons [6]. Therefore, it is likely that certain specific histaminergic compounds have potential clinical uses in preventing and treating ischemic stroke. However, histamine cannot cross the blood–brain barrier and it is involved in brain inflammation [7]. Carnosine (β-alanyl-L-histidine) is a naturally occurring dipeptide that is highly expressed in the central nervous system and can easily enter the brain from the periphery [8]. It has been assigned many putative roles, such as anti-inflammatory agent, free radical scavenger, and mobile organic pH buffer [9,10]. Carnosine protects against acute renal failure induced by ischemia/reperfusion in rats and NMDA-induced excitotoxic injury in differentiated PC12 cells through its conversion to histidine and histamine [11].

In addition, carnosine suppresses the extracellular glutamate level increase in excitotoxic insult in differentiated PC12 cells [12]. It also reverses the glutamate increase induced by morphine in the ventral tegmental area [13]. Recently, a line of study demonstrated that astrocytes, which take up carnosine, play an important role in maintaining low extracellular glutamate levels and eliminating and recycling glutamate in brain. Astrocytic glutamate transporter-1 (GLT-1) and glutamate/aspartate transporter (GLAST) are the primary controllers of extracellular glutamate levels in brain [14], and inhibition of GLT-1 and/or GLAST with pharmacological blockers or antisense oligonucleotides or by transgenic knockout elevates extracellular glutamate levels and induces neuronal death [3,15–17]. However, few reports have demonstrated significant relations between brain carnosine, histamine, and astrocyte-mediated glutamatergic signaling in ischemic stroke.

* Corresponding author. Fax: +86 571 88208413.
E-mail address: chenzhong@zju.edu.cn (Z. Chen).
[1] These authors contributed equally to this work.

0891-5849/$ – see front matter © 2009 Elsevier Inc. All rights reserved.
doi:10.1016/j.freeradbiomed.2009.12.021

Therefore, in this study, we asked whether the action of carnosine on ischemic stroke involves the histaminergic pathway or other mechanisms. We took advantage of the histidine decarboxylase knockout (HDC-KO) mouse, in which carnosine cannot be converted to histamine, to explore the role of carnosine in permanent middle cerebral artery occlusion (pMCAO) and the mechanisms involved in this action.

Materials and methods

Focal cerebral ischemia and drug treatment

All experiments using animals were performed in accordance with the National Institutes of Health *Guide for the Care and Use of Laboratory Animals*. Wild-type (WT) and HDC-KO male mice (C57BL/6 strain) weighing 22–30 g were used [18]. The HDC-KO mice were kindly provided by Professor Ohtsu. Focal cerebral ischemia was induced by pMCAO as previously described [19]. Mice were kept under sodium pentobarbital (60 mg/kg) anesthesia during the entire procedure and the rectal temperature was kept between 36.5 and 37.5°C using a Thermistor-controlled heated blanket. A 6-0 nylon monofilament suture, blunted at the tip and coated with 1% poly-L-lysine, was inserted into the right internal carotid artery and advanced until slight resistance was felt and a reduction in regional cerebral blood flow (rCBF) was seen. The rCBF, measured by a Perimed Periflux System 5000 laser Doppler perfusion monitor, dropped to 14.5 ± 0.6, 16.2 ± 0.6, 16.7 ± 0.6, 15.7 ± 0.5, and 17.7 ± 0.6 from 100% (baseline) soon after the onset of ischemia in the WT, WT + carnosine, WT + α-FMH + carnosine, KO, and KO + carnosine groups, respectively, and remained at that level throughout the occlusion period. Animals with less than 80% reduction in cerebral blood flow were excluded. The incision site was then closed and the animal was allowed to recover from anesthesia. Sham-operated mice were subjected to all steps described except for occlusion of the artery. Systolic blood pressure and heart rate were measured by a noninvasive tail cuff (ML 125; ADInstruments, Shanghai, China) connected to a PowerLab system. Arterial pO_2, pCO_2, and pH were monitored using an ABL700 radiometer (Leidu, Denmark).

Carnosine (Sigma) was dissolved in 9 g/L sterile saline (100 mg/ml) and administered by intraperitoneal injection. Saline or 250, 500, or 750 mg/kg carnosine was administered 30 min before ischemia. α-FMH (25 mg/kg; Merck Sharp & Dohme Research Laboratory, Rahway, NJ, USA) was injected intraperitoneally 3 h before carnosine administration in WT mice.

Neurological deficit scoring

Neurological deficit scores were evaluated 24 h after pMCAO, as described by Longa et al. [20]: 0, no deficit; 1, flexion of contralateral forelimb upon lifting of the whole animal by the tail; 2, circling to the contralateral side; 3, falling to the contralateral side; and 4, no spontaneous motor activity. Those mice that had an occlusion but did not show neurological deficits were excluded.

Evaluation of infarct volume

Animals were killed 24 h after ischemia. The brains were quickly removed, sectioned coronally at 2-mm intervals, and stained by immersion in the vital dye 2,3,5-triphenyltetrazolium hydrochloride (TTC; 0.25%) at 37°C for 30 min. The extent of the normal and infarcted areas was determined from digital images using ImageJ software. To compensate for the effect of brain edema, corrected infarct volumes were calculated as described by Chu et al. with slight modification: corrected infarct area = contralateral hemisphere area − (ipsilateral hemisphere area − measured infarct area) [21]. The infarct volume was calculated by summing the infarction areas of all sections and multiplying by slice thickness. The percentage of the corrected infarct was calculated by dividing the infarct volume by the total contralateral hemispheric volume, and this ratio was then multiplied by 100.

Primary cortical astrocyte cultures

Primary cortical astrocyte cultures were prepared from postnatal day 1–3 Sprague–Dawley rats as described previously [22]. Briefly, the cerebral cortices were digested with 0.25% trypsin for 20 min at 37°C, and then the dissociated cells were seeded onto poly-D-lysine-coated 75-cm^2 flasks. Cells were cultured in high-glucose DMEM (Gibco, USA) supplemented with 10% fetal bovine serum, 2 mM glutamine, 100 units/ml penicillin, and 100 mg/ml streptomycin. The cultures

Table 1
Effects of carnosine and α-FMH on physiological parameters before and after pMCAO in mice

Measurement	WT mice			KO mice	
	Saline	Carnosine	Carnosine + α-FMH	Saline	Carnosine
Blood pressure (mm Hg)					
Pre-pMCAO	150.6 ± 5.2	148.8 ± 5.2	155.7 ± 3.7	149.1 ± 5.0	148.7 ± 4.2
1 h after pMCAO	155.1 ± 7.1	152.8 ± 2.5	153.8 ± 2.4	147.8 ± 2.8	153.6 ± 4.6
Heart rate (beats/min)					
Pre-pMCAO	613.3 ± 26.0	590.0 ± 26.5	593.3 ± 17.6	610.0 ± 32.4	585.0 ± 28.8
1 h after pMCAO	620.0 ± 50.3	600.0 ± 17.3	600.0 ± 34.6	620.0 ± 53.0	595.0 ± 19.4
Temperature (°C)					
Pre-pMCAO	36.9 ± 0.2	37.1 ± 0.1	37.2 ± 0.1	36.8 ± 0.2	37.2 ± 0.1
1 h after pMCAO	37.1 ± 0.1	37.2 ± 0.2	37.1 ± 0.1	37.1 ± 0.2	37.0 ± 0.1
Blood pH					
Pre-pMCAO	7.28 ± 0.05	7.22 ± 0.04	7.23 ± 0.06	7.23 ± 0.06	7.3 ± 0.05
1 h after pMCAO	7.24 ± 0.03	7.22 ± 0.04	7.27 ± 0.06	7.29 ± 0.06	7.27 ± 0.02
pO_2 (mm Hg)					
Pre-pMCAO	125.9 ± 13.3	116.6 ± 4.4	113.4 ± 6.8	123.1 ± 6.8	120.8 ± 3.4
1 h after pMCAO	127.1 ± 7.1	111.1 ± 5.3	117.4 ± 1.9	114.1 ± 7.2	120.4 ± 9.7
pCO_2 (mm Hg)					
Pre-pMCAO	40.3 ± 3.5	40.3 ± 4.0	44.2 ± 4.9	38.0 ± 3.5	42.8 ± 1.8
1 h after pMCAO	42.7 ± 1.3	38.7 ± 2.1	43.1 ± 5.4	44.5 ± 3.0	44.2 ± 2.6

Carnosine (750 mg/kg) was administered intraperitoneally 30 min before ischemia. α-FMH (25 mg/kg) was injected intraperitoneally 3 h before carnosine administration in WT mice. Values are means ± SEM; $n = 3–5$ mice in each group.

were maintained at 37°C under >90% humidity and 5% CO_2. The medium was changed every 2–3 days until cells reached confluence. On days 10–14, the confluent cultures were shaken overnight to minimize microglia contamination. The remaining astrocyte monolayers were trypsinized and replated at a density of 2.5×10^4 cells/cm^2 onto 24- or 96-well plates or culture flasks. More than 95% of the cultured cells were astrocytes as identified by immunofluorescent staining for GFAP.

Oxygen–glucose deprivation and agent treatment

Oxygen–glucose deprivation (OGD) was performed as we previously described [23]. Briefly, astrocytes were washed twice and incubated in glucose-free DMEM (Gibco). Then the cultures were transferred into an anaerobic chamber filled with a gas mixture of 95% N_2/5% CO_2 at 37°C. In each experiment, cultures exposed to OGD were compared with normoxic controls supplied with DMEM containing glucose and maintained under standard incubation conditions. Cultures were treated with 5 mM carnosine for 30 min before OGD and it was present throughout the OGD process.

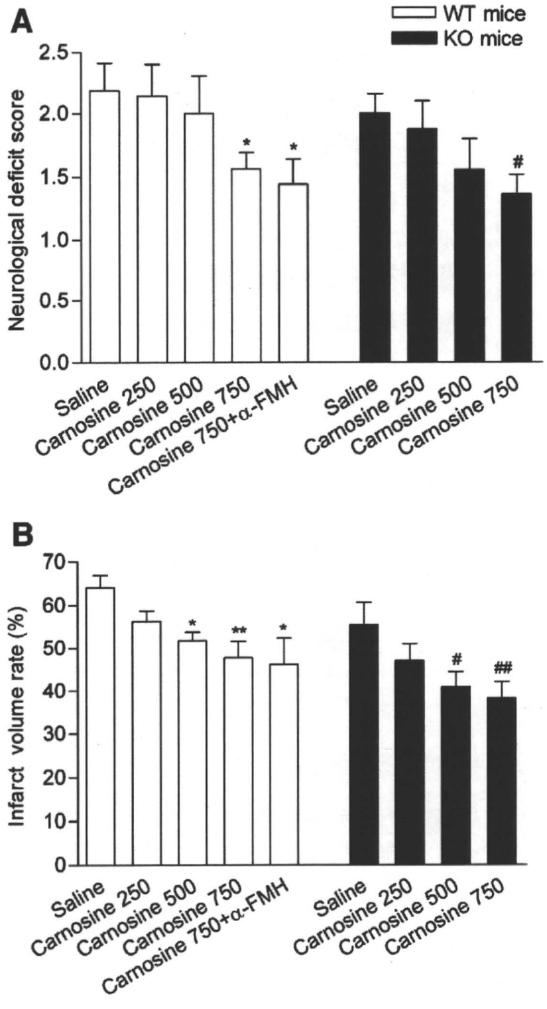

Fig. 1. Effects of carnosine and α-FMH on neurological function and infarct size in HDC-KO and WT mice at 24 h post-pMCAO. A single dose of carnosine administered intraperitoneally 30 min before ischemia (A) improved neurological function and (B) reduced infarct size in both HDC-KO and WT mice. α-FMH (25 mg/kg) injected intraperitoneally 3 h before carnosine did not reverse the protective action of carnosine on neurological function (A) or infarct size (B) in WT mice. Values show means ± SEM. $N = 69$; $^{*}P<0.05$ and $^{**}P<0.01$, compared with saline group in WT mice; $^{\#}P<0.05$ and $^{\#\#}P<0.01$, compared with saline group in HDC-KO mice.

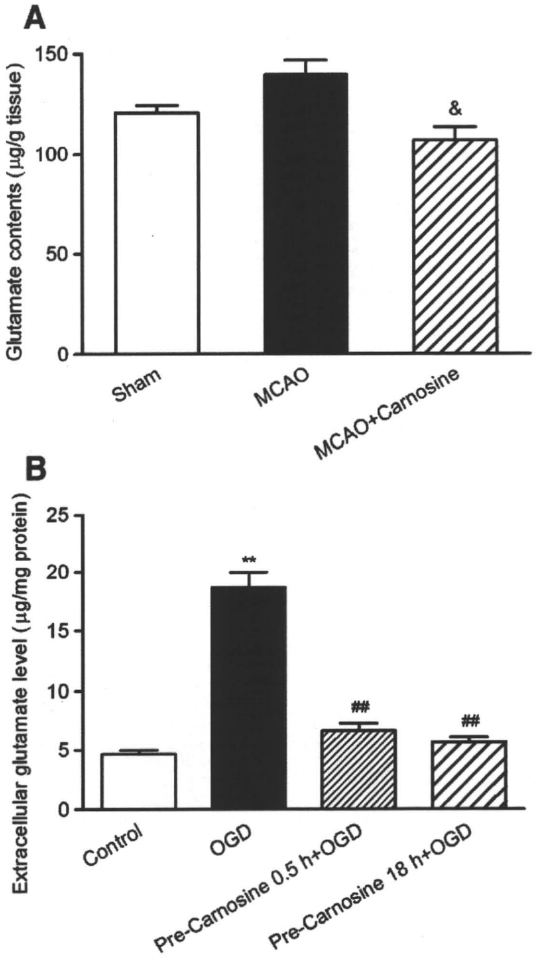

Fig. 2. Effects of carnosine on glutamate levels in ischemia in vivo and in vitro. (A) Carnosine (750 mg/kg) decreased glutamate content in the peri-infarct region in WT mice at 24 h post-pMCAO ($N = 18$). (B) Carnosine (5 mM) pretreatment for 0.5 or 18 h attenuated the increase in extracellular glutamate induced by OGD for 6 h in cultured cortical astrocytes. Values show means ± SEM. $^{\&}P<0.05$, compared with MCAO group; $^{**}P<0.01$, compared with control group; $^{\#\#}P<0.01$, compared with OGD group.

Neurochemical analysis of glutamate concentration

Mice were killed 24 h after pMCAO or sham operation, the brain was quickly removed, and the peri-infarct region in the ipsilateral cortex was dissected out and stored at −70°C until assay. In culture, samples of incubation solution were collected after OGD for 4 or 6 h, times at which no necrotic cell death was identified by propidium iodide (Molecular Probes, Eugene, OR, USA) staining. Analysis of glutamate in each sample was performed by high-performance liquid chromatography [24]. All of the equipment was from ESA (Chelmsford, MA, USA). After reacting with the derivate *o*-phthaladehyde, analysates were separated on a reversed-phase column (3 μm, 3×50 mm, Capcell Pak MG C18 column; Shiseido, Japan). A two-component gradient elution system was used, with component A of the mobile phase being 100 mM Na_2HPO_4, 13% acetonitrile, and 22% methanol, pH 6.8, and component B being the same as A except with 5.6% acetonitrile and 9.4% methanol. A gradient elution profile was used as follows: 0–3.5 min, isocratic 100% B; 3.5–20 min, linear ramp to 0% B; 20–22 min, isocratic 0% B; 22–23 min, linear ramp to 100% B; 23–30 min, isocratic 100% B. The temperature of the column was maintained at 38°C. The flow rate was set to 0.75 ml/min. The first cell was set at 250 mV, whereas the second cell was set at 550 mV.

Western blot analysis

Mice were killed 2 or 24 h after pMCAO or sham operation, the brain was quickly removed, and the peri-infarct region in the ipsilateral cortex was dissected out and lysed (Cell and Tissue Protein Extraction Solution; Kangchen). In culture, astrocytes were lysed after OGD for 6 h. Protein samples were separated by 12% SDS–polyacrylamide gel and then electrotransferred onto a nitrocellulose membrane. After being blocked with 5% fat-free milk, the membranes were incubated with goat polyclonal antibodies against GLAST and GLT-1 (1:50; Santa Cruz Biotechnology) and mouse monoclonal antibody against glyceraldehyde-3-phosphate dehydrogenase (GAPDH; 1:5000; Kangchen) at 4°C overnight. After repeated washes, the membranes were reacted with IRDye 800 anti-goat molecular probe (Odyssey; LI-COR) and IRDye 700 anti-mouse molecular probe (Odyssey; LI-COR) for 2 h. Images were acquired with the Odyssey infrared imaging system (Odyssey; LI-COR) and analyzed by the software program as specified in the Odyssey software manual. The results of expression were represented as the GLAST/GAPDH or GLT-1/GAPDH ratio and then were normalized to the values measured in the sham or control groups in vivo and in vitro, respectively (presented as 100%).

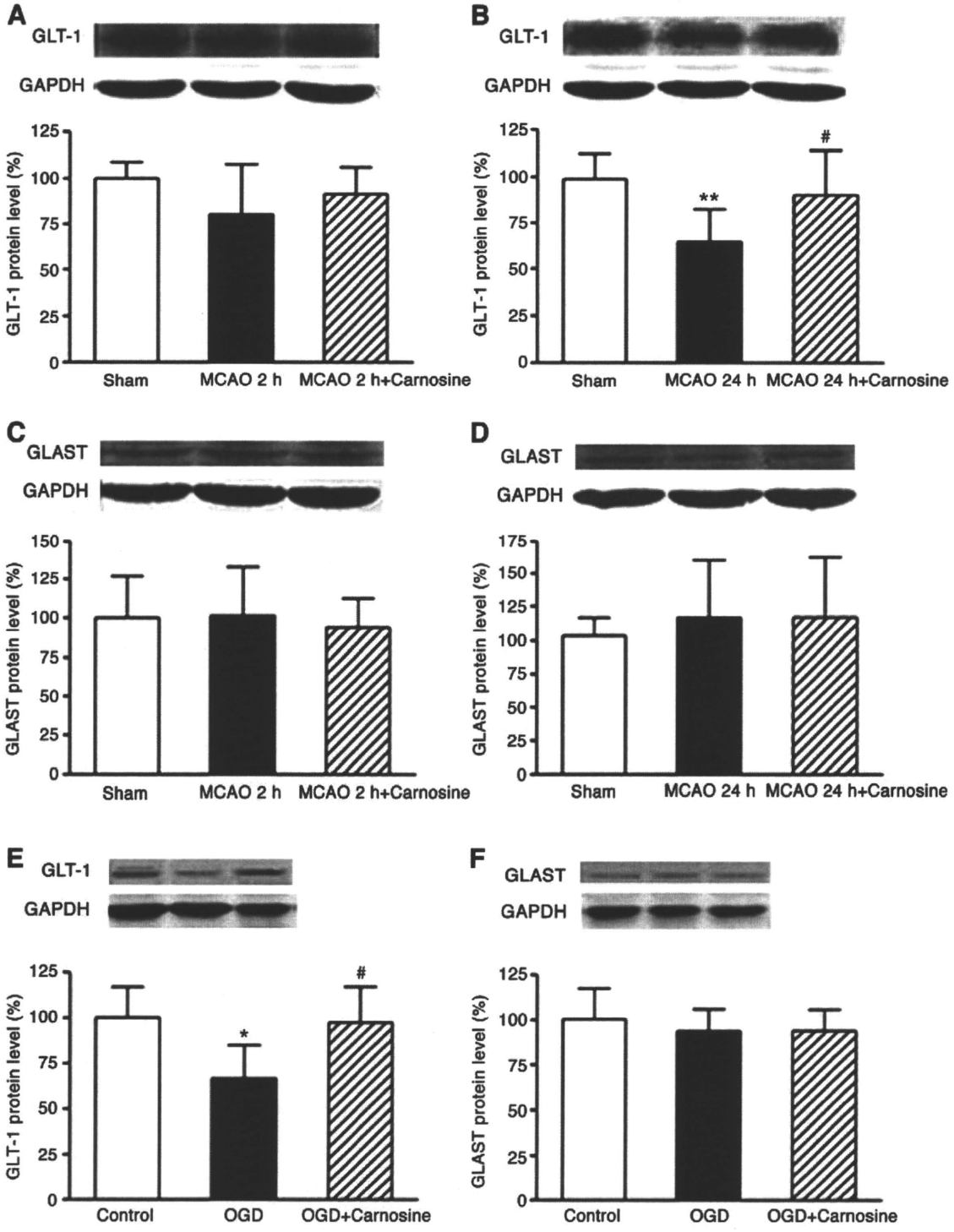

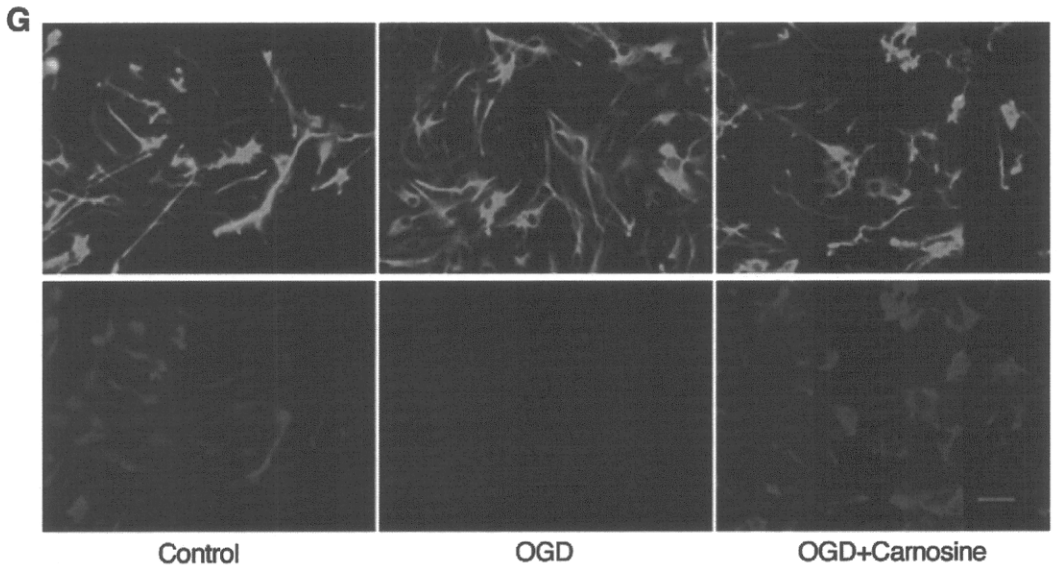

Fig. 3. Effects of ischemia and carnosine on the expression of GLT-1 and GLAST in vivo and in vitro. Western blot analysis of (A, B) GLT-1 and (C, D) GLAST protein levels in the peri-infarct region in WT mice at 2 or 24 h post-pMCAO or (E) GLT-1 and (F) GLAST in cultured cortical astrocytes exposed to OGD for 6 h. Values show means ± SEM. *$P<0.05$, **$P<0.01$, compared with sham or control group; #$P<0.05$ compared with pMCAO or OGD group. (G) Immunohistochemistry for GLT-1 expression in cultured astrocytes exposed to OGD for 6 h. Green, GFAP; red, GLT-1. Scale bar, 50 μm.

Immunohistochemistry

Immunostaining was also performed in cultured astrocytes as previously described [25]. Astrocytes seeded on coverslips were fixed in cold methanol for 10 min and incubated in 5% BSA for 2 h to block nonspecific binding of IgG. Then the cells were reacted with mouse monoclonal antibody against GFAP (1:400; Chemicon) at 4°C overnight. After being washed in PBS, astrocytes were reacted with guinea pig polyclonal antibody against GLAST or GLT-1 (1:2000; Chemicon) at 4°C overnight. After repeated washes, astrocytes were reacted with rhodamine-conjugated anti-guinea pig IgG-F(ab′)$_2$ antibody (1:100; Chemicon) and FITC-conjugated anti-mouse IgG antibody (1:100; Chemicon) for 2 h at room temperature. Finally, the stained cells were observed under a fluorescence microscope (Olympus BX51; Japan). In some experiments, the immunofluorescence intensity of GLT-1 was measured by ImageJ.

Mitochondrial reactive oxygen species measurement

Mitochondrial reactive oxygen species (ROS) were estimated using MitoSOX red (Molecular Probes), a specific mitochondrial superoxide ($O_2^{\bullet-}$) indicator. Cultures were incubated for 20 min at 37°C in the appropriate experimental medium containing MitoSOX (2 μM). After incubation, cultures were washed twice with fresh medium and kept in the second wash for microscopy. MitoSOX was visualized at 590 nm excitation and dye intensity was measured only in the cytoplasm as described previously [26].

Mitochondrial membrane potential assessment

The changes in relative mitochondrial membrane potential ($\Delta\Psi_m$) were assessed using the lipophilic cationic probe 5,5′,6,6′-tetrachloro-1,1′,3,3′-tetraethylbenzamid azolocarbocyanine iodide (JC-1; Molecular Probes). The dye JC-1 undergoes a reversible change in fluorescence emission from green to greenish orange as $\Delta\Psi_m$ increases. Cells with high $\Delta\Psi_m$ form JC-1 aggregates and fluoresce red; those with low $\Delta\Psi_m$ contain monomeric JC-1 and fluoresce green. After 6 h OGD, culture medium was removed and the cells, grown on coverslips, were incubated in the dark with JC-1 at a final concentration of 1.5 μM for 20 min. The cells were rinsed with PBS and excited at 488 nm with an Olympus BX-51 fluorescence microscope.

Statistical analysis

All data represent three or more independent experiments. Data are presented as means ± SEM. Statistical analyses were determined by SPSS 11.5 for Windows. One-way analysis of variance followed by LSD or Dunnett's T3 post hoc test (in which equal variances were not assumed) was used for multiple comparisons. Student's *t* test or the Mann–Whitney *U* test (when the data were not normally distributed) was used to analyze the significance of differences between the carnosine 750 mg/kg group and the carnosine 750 + α-FMH group. $P<0.05$ was considered statistically significant.

Results

Protective effect of carnosine on pMCAO is independent of the histaminergic pathway

To define the roles of carnosine and the carnosine–histidine–histamine metabolic pathway in pMCAO, we used the HDC-KO mouse, which lacks the histamine synthesis enzyme. Neither ischemia nor carnosine treatment had any effect on the physiological parameters of systolic blood pressure, heart rate, arterial pO_2, pCO_2, and pH when examined either before or 1 h after pMCAO in the HDC-KO and WT mice (Table 1). The neurological deficit scores were increased in both HDC-KO and WT mice 24 h after pMCAO and there was no significant difference between the two groups. Carnosine-treated (750 mg/kg) mice, both HDC-KO and WT, exhibited less profound deficits ($P<0.05$, Fig. 1A).

As assessed by TTC staining at 24 h post-pMCAO, the infarct volumes induced were 55.46 ± 5.16% in HDC-KO mice and 64.07 ± 2.86% in WT mice. Carnosine at 500 and 750 mg/kg markedly reduced the infarct size by 26.5% (40.78 ± 3.58%; $P<0.05$) and 31.07% (38.23 ± 3.77%; $P<0.01$) in HDC-KO mice and by 19.21% (51.76 ± 2.07%; $P<0.05$) and 25.46% (47.76 ± 3.90%; $P<0.01$) in WT mice, compared

with saline vehicle (Fig. 1B), and the degrees of neuroprotection exerted by carnosine in the two types of mice were not significantly different.

Moreover, α-FMH, a selective and irreversible inhibitor of histidine decarboxylase, which is the key enzyme in the synthesis of histamine from histidine, did not reverse the neuroprotective action of carnosine as shown by the neurological scores (carnosine group, 1.6 ± 0.1; carnosine + α-FMH group, 1.4 ± 0.2) and infarct volumes (carnosine group, 47.76 ± 3.90%; carnosine + α-FMH group, 46.16 ± 6.25%) in WT mice (Fig. 1).

Carnosine decreases glutamate levels after in vivo and in vitro ischemia

Glutamatergic synaptic dysfunction is the major mediator of excitotoxic neuronal death after focal cerebral ischemia. Here we determined the effects of carnosine on the glutamate levels in the peri-infarct region 24 h after pMCAO in WT mice and found that the glutamate content was lower in the carnosine-treated group (750 mg/kg) than in the saline group (carnosine-treated, 107.22 ± 6.61 μg/g tissue; saline, 142.2 ± 4.87 μg/g tissue; $P<0.05$; Fig. 2A).

Because of the fundamental roles of astrocytes in maintaining low extracellular glutamate levels and effective elimination and recycling of glutamate in brain, we took advantage of primary cultures of cortical astrocytes to examine, in greater detail, the effects of carnosine on extracellular glutamate levels induced by OGD. The extracellular glutamate did not increase significantly during OGD for 4 h (data not shown), but markedly increased at 6 h (300% increase; $P<0.01$). The OGD-induced increase in glutamate was suppressed by pretreatment with carnosine for 0.5 or 18 h (64.37 or 69.75% decrease, respectively, Fig. 2B).

Carnosine reverses GLT-1 decrease induced by in vivo and in vitro ischemia

To assess GLT-1 and GLAST after prolonged focal ischemia, we isolated the peri-infarct region 2 or 24 h post-pMCAO in WT mice. Western blot analysis showed that pMCAO for 2 h caused a slight decrease in GLT-1 (~70 kDa) expression (Fig. 3A), and a marked decrease in GLT-1 was induced by pMCAO for 24 h (33.94% decrease; $P<0.01$; Fig. 3B). However, expression of GLAST (~65 kDa) in the peri-infarct region was not changed by pMCAO for either 2 or 24 h (Figs. 3C and 3D). Carnosine pretreatment (750 mg/kg) reversed the decrease in GLT-1 expression 24 h after pMCAO. Similar results were obtained in HDC-KO mice (data not shown).

In vitro study also showed that GLT-1 but not GLAST expression in cortical astrocytes dramatically decreased after exposure to OGD for

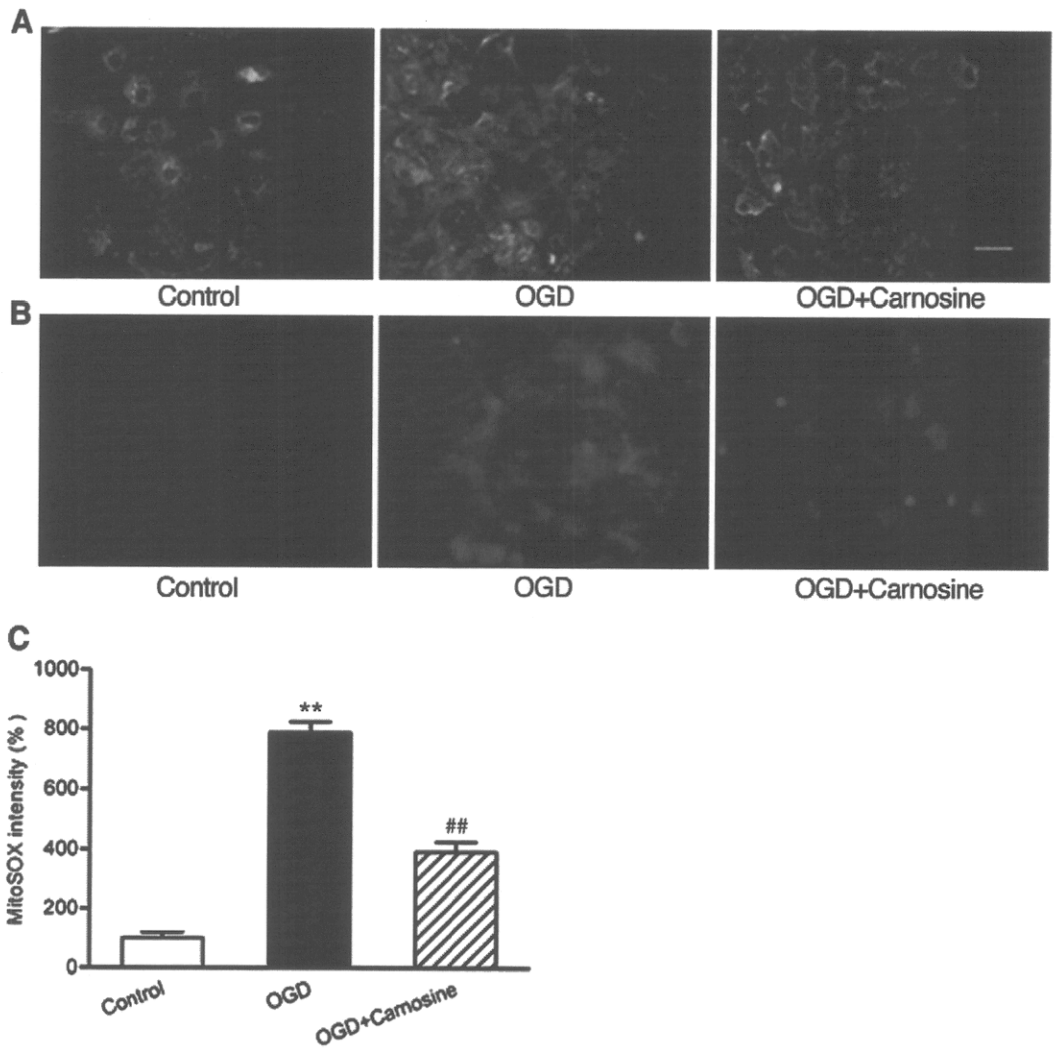

Fig. 4. Mitochondrial changes after OGD and carnosine treatment in cultured cortical astrocytes. (A) Changes in JC-1 fluorescence with 6 h OGD and carnosine treatment in cultured astrocytes. Red fluorescence indicates a polarized state and green fluorescence indicates a depolarized state. (B) Changes in ROS production indicated by MitoSOX fluorescence with 6 h OGD and carnosine treatment in cultured astrocytes. Scale bar, 50 μm. (C) Quantitative image analysis of MitoSOX fluorescence in cultured astrocytes at the end of OGD for 6 h. Values show means ± SEM. $^{**}P<0.01$, compared with control group; $^{\#\#}P<0.01$, compared with OGD group.

6 h. Carnosine treatment significantly prevented the decrease in GLT-1 expression, as assayed by Western blot analysis and immunohistochemistry (Figs. 3E, 3F, and 3G).

Mitochondrial dysfunction plays a crucial role in the regulation of GLT-1 expression in ischemic astrocytes

OGD for 6 h resulted in a significant dissipation of the $\Delta\Psi_m$ in cultured astrocytes (Fig. 4A). Pretreatment with carnosine for 0.5 h completely protected the dissipation of the $\Delta\Psi_m$ caused by OGD. The mitochondria of OGD-treated astrocytes were intensely stained by MitoSOX, with an ~7.9-fold increase in MitoSOX fluorescence intensity over control, whereas carnosine greatly suppressed (50%) the increase in MitoSOX intensity induced by OGD (Figs. 4B and 4C).

To further investigate the relationship between the expression of GLT-1 and mitochondrial function, we exposed the cultured astrocytes to rotenone, a specific inhibitor of mitochondrial respiratory complex I. Rotenone (2 μm) exposure for 6 h greatly increased the MitoSOX intensity and decreased the GLT-1 immunostaining at the same time. And pretreatment with carnosine markedly decreased the MitoSOX intensity and restored the GLT-1 expression (Fig. 5).

Discussion

In this study, we showed for the first time that carnosine ameliorated neurological dysfunction and reduced infarct size after pMCAO in HDC-KO and WT mice, to the same extent. Carnosine suppressed the mitochondrial ROS generation and $\Delta\Psi_m$ dissipation and therefore reversed the ischemia-induced decrease in GLT-1 expression in astrocytes and decreased glutamate levels in in vitro ischemia. These data suggest that the neuroprotective effect of carnosine on pMCAO in mice is not dependent on the histaminergic pathway, but may be due to a reduction in glutamate excitotoxicity via improved mitochondrial function in the ischemic brain.

We found that carnosine protected against the effects of pMCAO in both HDC-KO and WT mice. Carnosine serves as a non-mast-cell reservoir for histidine, utilized for the synthesis of histamine, which exerts neuroprotective effects on brain ischemia [4,12,27]. So it was proposed that carnosine may protect against pMCAO through the histaminergic pathway. However, surprisingly, carnosine significantly improved the neurological outcome and reduced the infarct size 24 h after pMCAO in both HDC-KO (31.07%) and WT mice (25.46%). Inhibition of histamine synthesis from carnosine by α-FMH did not

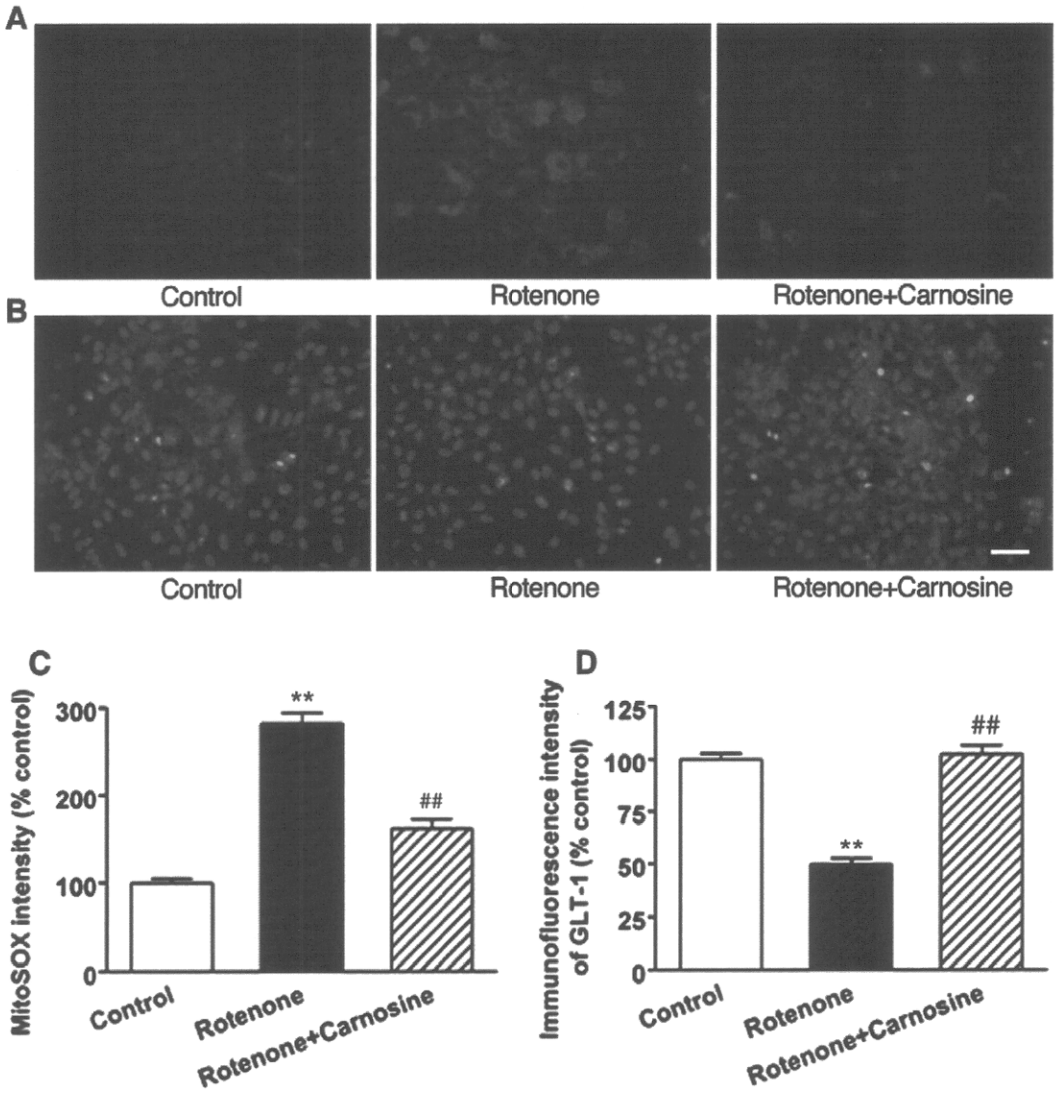

Fig. 5. Effects of rotenone and carnosine on the generation of mitochondrial ROS and GLT-1 expression in cultured cortical astrocytes. (A) Changes in ROS production induced by rotenone (2 μM) and carnosine (5 mM) in cultured astrocytes. (B) GLT-1 immunostaining in cultured astrocytes exposed to rotenone and carnosine. Red, GLT-1; blue, DAPI staining for nuclei. Scale bar, 50 μm. Quantitative image analysis of (C) MitoSOX fluorescence and (D) the immunofluorescence intensity of GLT-1 in cultured astrocytes at the end of rotenone (2 μM) exposure for 6 h. Values show means ± SEM. $^{**}P<0.01$, compared with control group; $^{\#\#}P<0.01$, compared with rotenone group.

reverse the protective action of carnosine in WT mice. These data demonstrated that carnosine has the same protective effect against ischemic injury whether or not mice lack histidine decarboxylase. In our previous study [12], we found that preincubation with carnosine caused a time-dependent synthesis of histamine and exerted maximal neuroprotection after preincubation for 18 h, when the histamine content reached the peak value in differentiated PC12 cells. However, in the present study, carnosine pretreatment for 0.5 or 18 h inhibited the extracellular glutamate level increase in astrocytes induced by OGD, to the same extent. This further confirms that the protective action of carnosine may not involve the carnosine–histidine–histamine metabolic pathway.

Previous studies showed a threefold increase in extracellular glutamate in the penumbra after 2 h of focal ischemia, which remains for several hours, and given a long enough permanent insult, both core and penumbra become infarcted and neuronal death occurs in the peri-infarct region [28]. Thus, it seems clinically meaningful to decrease the glutamate excitotoxicity and rescue the neurons in the peri-infarct region. Interestingly, we found that pretreatment with carnosine was capable of decreasing glutamate levels in the peri-infarct region 24 h post-pMCAO. Furthermore, we found that OGD for 6 h markedly increased extracellular glutamate levels in cultured cortical astrocytes, whereas carnosine significantly decreased the levels. But the question remained of how carnosine regulates glutamate levels. Because astrocytes are known to play an important role in glutamate uptake by GLT-1 and GLAST to limit excitotoxic injury of neighboring neurons [3], we further determined the effects of ischemia and carnosine on the expression of GLT-1 and GLAST. As shown in Fig. 3, we found that the expression of GLT-1 in cortical astrocytes was significantly decreased after pMCAO and OGD, but the expression of GLAST did not change appreciably. We do not know why only GLT-1 and not GLAST participates in this process. It may be because of their different distributions in the brain; for example, GLT-1 is predominantly localized in the cortex, whereas GLAST is mainly in the cerebellum [3]. Rao et al. also reported that transient MCAO leads to a delayed down-regulation of GLT-1, but not GLAST expression, in ischemic cortex [29]. So these data strongly suggest that cortical neurotoxicity induced by excessive extracellular glutamate may be mediated by GLT-1, but not GLAST. Furthermore, we found that pretreatment with carnosine increased the GLT-1 levels in astrocytes in the peri-infarct region 24 h post-pMCAO or in cultured astrocytes under OGD for 6 h, whereas it had no appreciable effect on GLAST. It is likely that carnosine acts by preserving the expression of GLT-1 in cortical astrocytes to regulate the uptake of extracellular glutamate and provide a much healthier environment for neuronal survival. However, we cannot rule out the possibility that carnosine also inhibits or delays the reversed operation of GLT-1 in brain ischemia, because GLT-1 can also run backward and release glutamate under severe ischemic conditions [30]. Further studies are required to resolve this point.

So far, the mechanisms of inhibiting GLT-1 expression in ischemic brain are obscure. Recently, Ouyang et al. [31] reported that mitochondrial dysfunction inhibits GLT-1 expression and leads to neurodegeneration after transient forebrain ischemia. It is proposed that mitochondrial dysfunction decreases the expression of cortical GLT-1 and then increases glutaminergic neurotoxic injury in ischemic brain. Here, we found that OGD markedly increased mitochondrial ROS and decreased $\Delta\Psi_m$ in cultured astrocytes, whereas expression of GLT-1 was significantly suppressed. Thus, our data provide further evidence that oxidative stress inhibits GLT-1 expression. In addition, we found that carnosine reversed the down-regulation of GLT-1 expression induced by OGD, as well as suppressing the increase in mitochondrial ROS and reversing the decrease in $\Delta\Psi_m$ in cultured astrocytes. We further exposed the cortical astrocytes to carnosine and rotenone and found that carnosine reversed the increase in ROS generation and decrease in GLT-1 expression induced by rotenone. Thus, these data indicate that the carnosine action on GLT-1 is probably attributable at least in part to its action on mitochondrial function, including suppression of mitochondrial ROS generation and $\Delta\Psi_m$ dissipation in astrocytes (Fig. 6). Our results are consistent with previous reports that carnosine protects PC12 cells from OGD-induced injury and protect rats, mice, and gerbils from damage induced by global ischemia or pMCAO, and such effects are partially due to the antioxidant activity [32–36]. However, contradictory results show that carnosine protects against excitotoxic cell death induced by kainate and NMDA in cerebellar granule cell neurons independent of

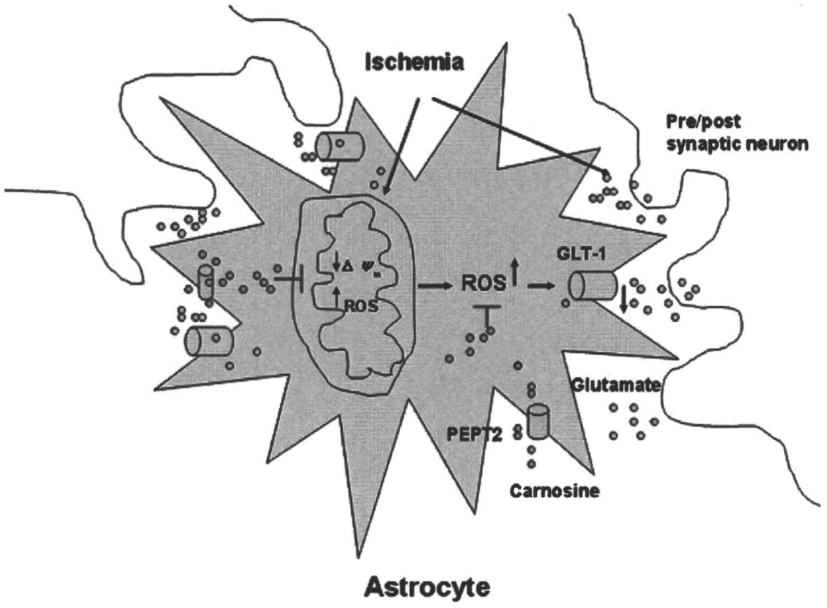

Fig. 6. Schematic showing hypothesized mechanisms underlying the carnosine action on cerebral ischemic excitotoxicity. Ischemia first induces mitochondrial ROS generation and dissipation of the $\Delta\Psi_m$ in cortical astrocytes, which leads to oxidative damage of GLT-1 on the astrocyte membrane and then increase of extracellular glutamate level. Carnosine suppresses the mitochondrial ROS generation and $\Delta\Psi_m$ dissipation and therefore alleviates the oxidative damage of GLT-1 and prevents glutamatergic excitotoxicity in ischemic brain.

its antioxidant effects [37]. These contradictory results are probably due to the different cell types and different types of insult in vitro and in vivo.

In conclusion, this study shows for the first time that carnosine is neuroprotective in pMCAO in HDC-KO and WT mice. And its action may not involve the carnosine–histidine–histamine metabolic pathway, but may work by reducing glutamate excitotoxicity by reversing the GLT-1 decrease in astrocytes induced by ischemia. These data suggest that carnosine may be a regulator of the astrocytic glutamate transporter to make it function optimally during ischemic stroke.

Acknowledgments

This project was supported by the National Natural Science Foundation of China (30725047, 30572176, 30801392, 30600757), by the National Basic Research of China 973 Program (2009CB521906), and partly by the New Century Excellent Talents Program, Ministry of Education, China (NCET-06-0511), the Zhejiang Province Healthy Excellent Youth Foundation, and the China Postdoctoral Science Foundation (20070420236). We are very grateful to Dr. Iain C. Bruce for reading the manuscript.

References

[1] Benveniste, H. The excitotoxin hypothesis in relation to cerebral ischemia. *Cerebrovasc. Brain Metab. Rev.* **3:**213–245; 1991.
[2] Rao, V. L.; Dogan, A.; Todd, K. G.; Bowen, K. K.; Kim, B. T.; Rothstein, J. D.; Dempsey, R. J. Antisense knockdown of the glial glutamate transporter GLT-1, but not the neuronal glutamate transporter EAAC1, exacerbates transient focal cerebral ischemia-induced neuronal damage in rat brain. *J. Neurosci.* **21:** 1876–1883; 2001.
[3] Rossi, D. J.; Brady, J. D.; Mohr, C. Astrocyte metabolism and signaling during brain ischemia. *Nat. Neurosci.* **10:**1377–1386; 2007.
[4] Hamami, G.; Adachi, N.; Liu, K.; Arai, T. Alleviation of ischemic neuronal damage by histamine H2 receptor stimulation in the rat striatum. *Eur. J. Pharmacol.* **484:** 167–173; 2004.
[5] Adachi, N.; Oishi, R.; Itano, Y.; Yamada, T.; Hirakawa, M.; Saeki, K. Aggravation of ischemic neuronal damage in the rat hippocampus by impairment of histaminergic neurotransmission. *Brain Res.* **602:**165–168; 1993.
[6] Dai, H.; Zhang, Z.; Zhu, Y.; Shen, Y.; Hu, W.; Huang, Y.; Luo, J.; Timmerman, H.; Leurs, R.; Chen, Z. Histamine protects against NMDA-induced necrosis in cultured cortical neurons through H receptor/cyclic AMP/protein kinase A and H receptor/GABA release pathways. *J. Neurochem.* **96:**1390–1400; 2006.
[7] Vizuete, M. L.; Merino, M.; Venero, J. L.; Santiago, M.; Cano, J.; Machado, A. Histamine infusion induces a selective dopaminergic neuronal death along with an inflammatory reaction in rat substantia nigra. *J. Neurochem.* **75:** 540–552; 2000.
[8] Bakardjiev, A.; Bauer, K. Biosynthesis, release, and uptake of carnosine in primary cultures. *Biochemistry (Moscow)* **65:**779–782; 2000.
[9] Boldyrev, A. A. Problems and perspectives in studying the biological role of carnosine. *Biochemistry (Moscow)* **65:**751–756; 2000.
[10] Marchis, S. D.; Modena, C.; Peretto, P.; Migheli, A.; Margolis, F. L.; Fasolo, A. Carnosine-related dipeptides in neurons and glia. *Biochemistry (Moscow)* **65:** 824–833; 2000.
[11] Kurata, H.; Fujii, T.; Tsutsui, H.; Katayama, T.; Ohkita, M.; Takaoka, M.; Tsuruoka, N.; Kiso, Y.; Ohno, Y.; Fujisawa, Y.; Shokoji, T.; Nishiyama, A.; Abe, Y.; Matsumura, Y. Renoprotective effects of L-carnosine on ischemia/reperfusion-induced renal injury in rats. *J. Pharmacol. Exp. Ther.* **319:**640–647; 2006.
[12] Shen, Y.; Hu, W. W.; Fan, Y. Y.; Dai, H. B.; Fu, Q. L.; Wei, E. Q.; Luo, J. H.; Chen, Z. Carnosine protects against NMDA-induced neurotoxicity in differentiated rat PC12 cells through carnosine–histidine–histamine pathway and H(1)/H(3) receptors. *Biochem. Pharmacol.* **73:**709–717; 2007.
[13] Gong, Y. X.; Wang, H. J.; Zhu, Y. P.; Zhang, W. P.; Dai, H. B.; Zhang, S. H.; Wei, E. Q.; Chen, Z. Carnosine ameliorates morphine-induced conditioned place preference in rats. *Neurosci. Lett.* **422:**34–38; 2007.
[14] Sun, X. L.; Zeng, X. N.; Zhou, F.; Dai, C. P.; Ding, J. H.; Hu, G. KATP channel openers facilitate glutamate uptake by GluTs in rat primary cultured astrocytes. *Neuropsychopharmacology* **33:**1336–1342; 2008.
[15] Mitani, A.; Tanaka, K. Functional changes of glial glutamate transporter GLT-1 during ischemia: an in vivo study in the hippocampal CA1 of normal mice and mutant mice lacking GLT-1. *J. Neurosci.* **23:**7176–7182; 2003.
[16] Rothstein, J. D.; Dykes-Hoberg, M.; Pardo, C. A.; Bristol, L. A.; Jin, L.; Kuncl, R. W.; Kanai, Y.; Hediger, M. A.; Wang, Y.; Schielke, J. P.; Welty, D. F. Knockout of glutamate transporters reveals a major role for astroglial transport in excitotoxicity and clearance of glutamate. *Neuron* **16:**675–686; 1996.
[17] Izumi, Y.; Shimamoto, K.; Benz, A. M.; Hammerman, S. B.; Olney, J. W.; Zorumski, C. F. Glutamate transporters and retinal excitotoxicity. *Glia* **39:**58–68; 2002.
[18] Ohtsu, H.; Tanaka, S.; Terui, T.; Hori, Y.; Makabe-Kobayashi, Y.; Pejler, G.; Tchougounova, E.; Hellman, L.; Gertsenstein, M.; Hirasawa, N.; Sakurai, E.; Buzas, E.; Kovacs, P.; Csaba, G.; Kittel, A.; Okada, M.; Hara, M.; Mar, L.; Numayama-Tsuruta, K.; Ishigaki-Suzuki, S.; Ohuchi, K.; Ichikawa, A.; Falus, A.; Watanabe, T.; Nagy, A. Mice lacking histidine decarboxylase exhibit abnormal mast cells. *FEBS Lett.* **502:**53–56; 2001.
[19] Yu, G. L.; Wei, E. Q.; Wang, M. L.; Zhang, W. P.; Zhang, S. H.; Weng, J. Q.; Chu, L. S.; Fang, S. H.; Zhou, Y.; Chen, Z.; Zhang, Q.; Zhang, L. H. Pranlukast, a cysteinyl leukotriene receptor-1 antagonist, protects against chronic ischemic brain injury and inhibits the glial scar formation in mice. *Brain Res.* **1053:**116–125; 2005.
[20] Longa, E. Z.; Weinstein, P. R.; Carlson, S.; Cummins, R. Reversible middle cerebral artery occlusion without craniectomy in rats. *Stroke* **20:**84–91; 1989.
[21] Chu, K.; Lee, S. T.; Sinn, D. I.; Ko, S. Y.; Kim, E. H.; Kim, J. M.; Kim, S. J.; Park, D. K.; Jung, K. H.; Song, E. C.; Lee, S. K.; Kim, M.; Roh, J. K. Pharmacological induction of ischemic tolerance by glutamate transporter-1 (EAAT2) upregulation. *Stroke* **38:** 177–182; 2007.
[22] Ciccarelli, R.; D'Alimonte, I.; Ballerini, P.; D'Auro, M.; Nargi, E.; Buccella, S.; Di Iorio, P.; Bruno, V.; Nicoletti, F.; Caciagli, F. Molecular signalling mediating the protective effect of A1 adenosine and mGlu3 metabotropic glutamate receptor activation against apoptosis by oxygen/glucose deprivation in cultured astrocytes. *Mol. Pharmacol.* **71:**1369–1380; 2007.
[23] Shen, Y.; Zhang, S.; Fu, L.; Hu, W.; Chen, Z. Carnosine attenuates mast cell degranulation and histamine release induced by oxygen-glucose deprivation. *Cell. Biochem. Funct.* **26:**334–338; 2008.
[24] Jin, C. L.; Yang, L. X.; Wu, X. H.; Li, Q.; Ding, M. P.; Fan, Y. Y.; Zhang, W. P.; Luo, J. H.; Chen, Z. Effects of carnosine on amygdaloid-kindled seizures in Sprague–Dawley rats. *Neuroscience* **135:**939–947; 2005.
[25] Huang, X. J.; Zhang, W. P.; Li, C. T.; Shi, W. Z.; Fang, S. H.; Lu, Y. B.; Chen, Z.; Wei, E. Q. Activation of CysLT receptors induces astrocyte proliferation and death after oxygen–glucose deprivation. *Glia* **56:**27–37; 2008.
[26] Kirkland, R. A.; Saavedra, G. M.; Franklin, J. L. Rapid activation of antioxidant defenses by nerve growth factor suppresses reactive oxygen species during neuronal apoptosis: evidence for a role in cytochrome c redistribution. *J. Neurosci.* **27:**11315–11326; 2007.
[27] Adachi, N. Cerebral ischemia and brain histamine. *Brain Res. Brain Res. Rev.* **50:** 275–286; 2005.
[28] Lipton, P. Ischemic cell death in brain neurons. *Physiol. Rev.* **79:**1431–1568; 1999.
[29] Rao, V. L.; Bowen, K. K.; Dempsey, R. J. Transient focal cerebral ischemia down-regulates glutamate transporters GLT-1 and EAAC1 expression in rat brain. *Neurochem. Res.* **26:**497–502; 2001.
[30] Takahashi, M.; Billups, B.; Rossi, D.; Sarantis, M.; Hamann, M.; Attwell, D. The role of glutamate transporters in glutamate homeostasis in the brain. *J. Exp. Biol.* **200:** 401–409; 1997.
[31] Ouyang, Y. B.; Volobouéva, L. A.; Xu, L. J.; Giffard, R. G. Selective dysfunction of hippocampal CA1 astrocytes contributes to delayed neuronal damage after transient forebrain ischemia. *J. Neurosci.* **27:**4253–4260; 2007.
[32] Dobrota, D.; Fedorova, T.; Stvolinsky, S.; Babusikova, E.; Likavcanova, K.; Drgova, A.; Strapkova, A.; Boldyrev, A. Carnosine protects the brain of rats and Mongolian gerbils against ischemic injury: after-stroke-effect. *Neurochem. Res.* **30:** 1283–1288; 2005.
[33] Gallant, S.; Kukley, M.; Stvolinsky, S.; Bulygina, E.; Boldyrev, A. Effect of carnosine on rats under experimental brain ischemia. Tohoku. *J. Exp. Med.* **191:**85–99; 2000.
[34] Stvolinsky, S. L.; Dobrota, D. Anti-ischemic activity of carnosine. *Biochemistry (Moscow)* **65:**849–855; 2000.
[35] Rajanikant, G. K.; Zemke, D.; Senut, M. C.; Frenkel, M. B.; Chen, A. F.; Gupta, R.; Majid, A. Carnosine is neuroprotective against permanent focal cerebral ischemia in mice. *Stroke* **38:**3023–3031; 2007.
[36] Tabakman, R.; Lazarovici, P.; Kohen, R. Neuroprotective effects of carnosine and homocarnosine on pheochromocytoma PC12 cells exposed to ischemia. *J. Neurosci. Res.* **68:**463–469; 2002.
[37] Boldyrev, A.; Song, R.; Lawrence, D.; Carpenter, D. O. Carnosine protects against excitotoxic cell death independently of effects on reactive oxygen species. *Neuroscience* **94:**571–577; 1999.

Involvement of prostaglandins and histamine in nickel wire-induced acute inflammation in mice

Noriyasu Hirasawa,[1,2] Yoshiaki Goi,[2] Rina Tanaka,[1] Kenji Ishihara,[2,3] Hiroshi Ohtsu,[4] Kazuo Ohuchi[2,5]

[1]*Laboratory of Pharmacotherapy of Life-Style Related Diseases, Graduate School of Pharmaceutical Sciences, Tohoku University, Sendai 980-8578, Japan*

[2]*Laboratory of Pathophysiological Biochemistry, Graduate School of Pharmaceutical Sciences, Tohoku University, Sendai 980-8578, Japan*

[3]*Course for School Nurse Teacher, Faculty of Education, Ibaraki University, Mito 310-8512, Japan*

[4]*Department of Quantum Science and Energy Engineering, Graduate School of Engineering, Tohoku University, Sendai 980-8579, Japan*

[5]*Laboratory of Life Sciences, Faculty of Pharmacy, Yasuda Women's University, Hiroshima 731-0153, Japan*

Received 7 March 2009; revised 28 July 2009; accepted 5 August 2009
Published online 16 October 2009 in Wiley InterScience (www.interscience.wiley.com). DOI: 10.1002/jbm.a.32628

Abstract: The irritancy of Nickel (Ni) ions has been well documented clinically. However, the chemical mediators involved in the acute inflammation induced by solid Ni are not fully understood. We used the Ni wire-implantation model in mice and examined roles of prostaglandins and histamine in plasma leakage in the acute phase. The subcutaneous implantation of a Ni wire into the back of mice induced plasma leakage from 8 to 24 h and tissue necrosis around the wire at 3 days, whereas the implantation of an aluminum wire induced no such inflammatory responses. An increase in the mRNA for cyclooxygenase (COX)-2 and HDC in cells around the Ni wire was detected 4 h after the implantation. The leakage of plasma at 8 h was inhibited by indomethacin in a dose-dependent manner. Dexamethasone and the p38 MAP kinase inhibitor SB203580 also inhibited the exudation of plasma consistent with the inhibition of the expression of COX-2 mRNA. Furthermore, plasma leakage was partially but siginificantly reduced in histamine H1 receptor knockout mice and histidine decarboxylase (HDC) knockout mice but not in H2 receptor knockout mice. These results suggested that the Ni ions released from the wire induced the expression of COX-2 and HDC, resulting in an increase in vascular permeability during the acute phase of inflammation. © 2009 Wiley Periodicals, Inc. J Biomed Mater Res 93A: 1306–1311, 2010

Key words: Ni; inflammation; vascular permeability; prostaglandin; histamine

INTRODUCTION

Since nickel (Ni) has especially high irritancy and allergenicity among metals,[1] nickel (Ni) ions released from accessories, coins, and biomaterials can cause local inflammation and allergies.[2–4] Ni in alloys attached to skin or implanted in the body is eluted in sweat or tissue fluid. The Ni ions form complexes with proteins such as serum albumin and membrane proteins on the surface of cells,[5] and induce a delayed-type hypersensitivity reaction.[6–8] However, in contrast with such immunological responses, the acute inflammation induced by the ions released from solid Ni is not well understood.

Correspondence to: N. Hirasawa; e-mail: hirasawa@mail.pharm.tohoku.ac.jp

Contract grant sponsor: The Cosmetology Research Foundation

There are relatively few reports about animal models of Ni-induced inflammation. A metal wire or plate has been implanted into rats or guinea pigs to evaluate the toxicity or safety of alloys used in surgery and orthopedical procedures.[3,4] In the Ni wire-implantation model in rats, Wataha et al. determined the concentration of Ni ions by the laser-ablation technique at 7 days and demonstrated that the distribution of Ni in tissues correlated well with inflammation.[9] However, the molecular mechanisms by which solid Ni induces inflammation were not clarified.

Prostaglandin (PG) E_2 and histamine are well-known chemical mediators of inflammation. We have reported roles for these mediators in models of inflammation induced by carrageenin,[10] antigens,[11,12] and cotton thread.[13] In human dermatitis caused by Ni, an increase in the concentration of PGE2 in the skin was observed.[14] The biosynthesis of PGE2 is regulated in three steps; (1) the release of arachidonic acid by phospholipase A2, (2) the conversion

of arachidonic acid to PGH2 by cyclooxygenase (COX), and (3) the conversion of PGH2 to PGE2 by PGE synthase. COX-1 is constitutively expressed in most tissues while the expression of COX-2 is induced by inflammatory stimuli.[15] Thus, the production of PGs in inflamed tissues is mainly regulated by the expression of COX-2. Histamine is, in general, released by mast cells through IgE-mediated stimulation by an antigen. In addition, a histamine-producing enzyme, histidine decarboxylase (HDC), is produced in inflammatory cells such as neutrophils and macrophages in the acute phase and chronic phase of inflammation.[13,16] IgE-independent production is another source of histamine, along with anaphylactic release from mast cells. Ni-sensitized mice challenged with Ni ions showed an increase in HDC activity in parallel with ear swelling,[17] indicating the histamine produced to also be involved in vascular permeability. Thus the expression of COX-2 and HDC are good markers of the production of PGs and histamine at the inflamed sites.

In this study, we established a Ni wire-induced inflammation model to clarify how solid Ni induces inflammatory responses, and examined the involvement of prostaglandins and histamine in the leakage of plasma during acute inflammation.

MATERIALS AND METHODS

Animals

Male C57BL/6 mice, specific pathogen free and weighing 22–25 g, were purchased from Charles River. Histamine H1 receptor knockout mice[18] and H2 receptor knockout mice,[19] backcrossed to C57BL/6 for six generations were provided by Prof. Watanabe at Kyushu University. HDC knockout mice[20] were backcrossed to C57BL/6 for six generations. The mice were treated in accordance with procedures approved by the Animal Ethics Committee of Tohoku University, Japan.

Implantation of metal wires

A Ni wire (99.35%, φ 0.8 mm), iron (Fe) wire (99.5%, φ 0.8 mm), Aluminum (Al) wire (99.99%, φ 0.8 mm), and cobalt (Co) wire (99.99%, φ 0.5 mm) (Nilako, Tokyo, Japan) were cut into length of 5 mm in length and sterilized with dry heat at 160°C for 2 h. Mice were anesthetized and a length of wire was implanted subcutaneously in the dorsum using a 13G implant needle (Natsume, Tokyo, Japan).

Macroscopic and histochemical analysis

Mice were sacrificed 0, 8, 24 h, or 3 days after the implantation. The skin was removed for macroscopic observation. Tissue including skin, the cutaneous muscle layer, and subcutaneous tissue on the wire was then excised. The excised tissue was fixed in 10% (v/v) formalin in PBS for 72 h at 4°C and processed for paraffin embedding. The tissue sections (5 μm) were stained with hematoxylin and eosin.

Quantitative analysis of plasma exudation

The mice were injected intravenously with 0.2 mL of a 0.5% (w/v) Evans blue solution via the tail at a specified time. Thirty minutes after the injection, the mice were sacrificed and tissue (14 mm in diameter) including skin, the cutaneous muscle layer, and subcutaneous tissue on the wire was excised. The tissue was minced and soaked in 0.5 mL of extraction solution (Acetone: 0.5% Na_2SO_4 solution = 7:3). After incubation for 24 h at room temperature, each sample was centrifuged for 10 min at 1500*g* and 4°C and the absorbance at 595 nm of the supernatant was determined.

Drug administration

Dexamethasone (Sigma-Aldrich, St Louis, MO) and indomethacin (Wako Pure Chemical Ind., Osaka, Japan) were suspended in a 0.5% (w/v) sodium carboxymethylcellulose solution. The mice were orally administered dexamethasone (0.15 and 1.5 mg/kg) or indomethacin (1, 3, and 10 mg/kg) 3 or 1 h before the implantation of the Ni wire, respectively. The p38 MAP kinase inhibitor SB203580 (Calbiochem-Novabiochem, San Diego, CA) was dissolved in DMSO, diluted in 100 μL of saline, and then injected into the site of implantation of the Ni wire just after the implantation. Sham control mice received the same amount of saline containing 1% DMSO.

Semi-quantitative analysis of COX-2 and HDC mRNA at the inflamed site

Tissue (3 mm × 5 mm) including the skin, cutaneous muscle layer, and subcutaneous tissues adjacent to the Ni wire was excised 4 h or at the indicated time after the implantation and frozen in liquid nitrogen. The tissue was crushed into pieces using a SK mill (Tokken, Chiba, Japan), and total RNA was prepared with a GenElute™ Mammalian Total RNA Kit (Sigma-Aldrich) according to the manufacturer's instructions. The yield of RNA extracted was determined by spectrophotometry. The RNA (0.3 μg) was reverse-transcribed at 37°C for 1 h by adding 50 ng of random primer (Invitrogen), 200 units of M-MLV reverse transcriptase (Invitrogen), 10 n*M* deoxyribonucleotide triphosphates (dNTP) (Takara, Otsu, Japan), 10 m*M* dithiothreitol (Invitrogen), and 40 units of RNaseOUT™ (Invitrogen). The primers used were 5′-TTG AAG ACC AGG AGT ACA GC-3′ (sense) and 5′-GGT ACA GTT CCA TGA CAT CG-3′ (antisense) for COX-2, 5′-GGA TCC AAG ATC AGA TTT CTA CCT GTG GAC-3′ (sense) and 5′-GTC GAC GAC ATG TGC TTG AAG ATT CTT CAC-3′

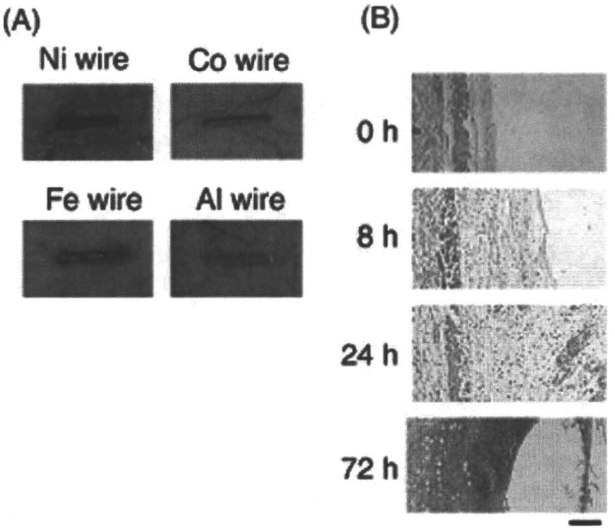

Figure 1. Ni wire-induced inflammation in mice (A) A Ni, Co, Fe, or Al wire was implanted subcutaneously in the dorsum of C57BL/6 mice. The mice were sacrificed 3 days after the implantation, and the inflamed site was photographed. (B) A Ni wire was implanted subcutaneously in the dorsum, and mice were sacrificed 0, 8, 24, and 72 h later. Paraffin sections of the tissue surrounding the implanted wire were prepared and stained with hematoxylin and eosin. Scale bars indicated 100 μm. [Color figure can be viewed in the online issue, which is available at www.interscience.wiley.com.]

(antisense) for HDC, and 5′-TGA TGA CAT CAA GAA GGT GGT GGA-3′ (sense) and 5′-TCC TTG GAG GCC ATG TAG GCC AT-3′ (antisense) for glyceraldehyde-3-phosphate dehydrogenase (GAPDH). The PCR for COX-2 was performed for 34 cycles of 94°C for 0.5 min, 52°C for 0.5 min, and 72°C for 0.5 min, that for HDC for 30 cycles of 94°C for 0.5 min, 56°C for 1 min, and 72°C for 2 min, and that for GAPDH for 30 cycles of 94°C for 0.5 min, 57°C for 1 min, and 72°C for 2 min. The reaction mixture (10 μL) was subjected to electrophoresis on a 2% agarose gel, and visualized by ethidium bromide staining. The levels of mRNA for COX-2, HDC and GAPDH were quantified by scanning densitometry.

RESULTS

A metal wire-induced inflammation in mice

A Ni, Co, Fe, or Al wire was implanted subcutaneously into the dorsum of C57BL/6 mice and the response was observed 3 days later. The Ni wire caused extreme inflammation but the Co, Fe, and Al wires did not [Fig. 1(A)]. Edema and infiltration of leukocytes were observed 8 h after the implantation, and these responses were markedly increased at 24 h [Fig. 1(B)]. At 3 days, necrosis was observed around the Ni wire [Fig. 1(B)].

Ni wire-induced plasma exudation

The amount of Evans blue that leaked in a 30-min period was determined 4, 8, and 24 h after the implantation of the Ni or Al wire. A quantitative analysis revealed that the Ni wire significantly increased plasma leakage from 8 to 24 h (Fig. 2). In contrast, the Al wire did not increase plasma leakage during the experimental periods (Fig. 2).

Induction of COX-2 mRNA and HDC mRNA expression by the Ni wire

To clarify whether prostaglandins and histamine were produced following implantation of the Ni wire, the expression of COX-2 mRNA and HDC mRNA was examined. The level of COX-2 mRNA at 4 h was significantly increased by the implantation of the Ni wire but not by the Al wire [Fig. 3(A)]. The expression of HDC mRNA was also detected 4 h after implantation of the Ni wire [Fig. 3(B)] but not 4 h after implantation of the Al wire (data not shown).

Effect of anti-inflammatory drugs on the Ni wire-induced plasma exudation

To clarify the involvement of COX-2 and prostaglandins in the leakage of plasma during the acute phase of Ni-induced inflammation, the effects of the

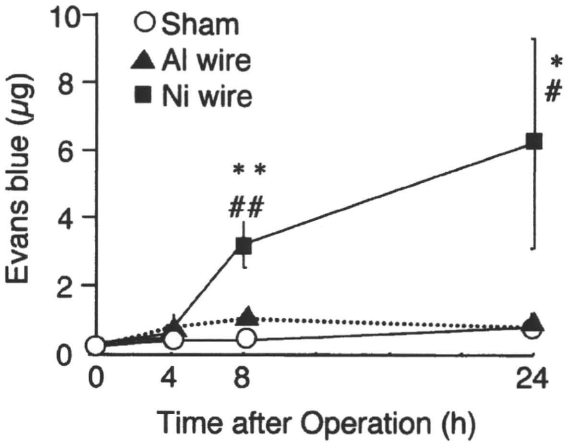

Figure 2. Plasma exudation induced by Ni and Al wires A Ni or Al wire was implanted subcutaneously in the dorsum of mice. The animals were injected intravenously with 0.2 mL of a 0.5% (w/v) Evans blue solution 4, 8, or 24 h after the implantation. Thirty minutes later, they were sacrificed and the skin was dissected. The Evans blue in the tissue (diameter: 14 mm) was extracted and quantified by colorimetric analysis. Values are means for three or four mice with the SEM shown by vertical bars. Statistical significance; $^{*}p < 0.05$, $^{**}p < 0.01$ vs. the sham operation group at the corresponding time point, and $^{\#}p < 0.05$, $^{\#\#}p < 0.01$ vs. the Al wire implantation group at the corresponding time point.

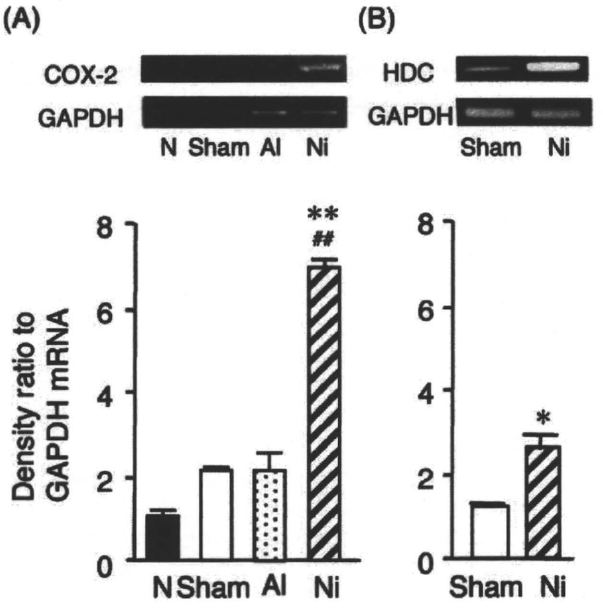

Figure 3. Effects of the implantation on the expression of COX-2 and HDC mRNA in tissue surrounding the wire A Ni or Al wire was implanted subcutaneously in the dorsum of mice. Four hours later, the skin tissues (3 mm × 5 mm) including the cutaneous muscle layer and subcutaneous tissue adjacent to the wire were excised. Total RNA was extracted from the excised tissue and the levels of mRNA for COX-2 (A) and HDC (B) were determined by RT-PCR. The level of mRNA for COX-2 was quantified by scanning densitometry, and the density ratio of COX-2 mRNA or HDC mRNA to GAPDH mRNA was calculated. The value for untreated skin tissue is set to 1.0. The values are means for two or three mice with the SEM shown by vertical bars. Statistical significance; $^{**}p < 0.01$ vs. the sham operation group, and $^{\#\#}p < 0.01$ vs. the Al wire implantation group in C57BL/6 mice. N: no treatment, Sham: sham operation, Al and Ni: implantation of Al and Ni wire, respectively.

cyclooxygenase inhibitor indomethacin, the steroidal anti-inflammatory drug dexamethasone, and the inhibitor of p38 MAP kinase SB203580 were examined. Indomethacin and dexamethasone prevented plasma from leaking in the 30-min period from 8 to 8.5 h after the implantation in a dose-dependent manner. SB203580 (100 μM) injected adjacent to the wire just after its implantation also significantly inhibited any leakage [Fig. 4(A)]. Dexamethasone and SB203580 reduced the level of COX-2 mRNA in tissue adjacent to the wire excised 4 h postimplantation, although indomethacin did not [Fig. 4(B)].

Plasma leakage in histamine receptor-deficient mice

The Ni wire was implanted subcutaneously in the dorsum of histamine H1 receptor knockout mice, H2 receptor knockout mice and HDC knockout mice and the leakage of plasma from 8 to 8.5 h was determined. As shown in Figure 5, the leakage was attenuated partially but significantly in H1 receptor knockout mice and HDC knockout mice, but not changed in H2 receptor knockout mice.

DISCUSSION

In this study, we developed an animal model of contact dermatitis by implanting a Ni wire in mice. We found that the wire triggered extensive induced inflammation and that PGs and histamine were involved in the leakage of the plasma early in the inflammatory process.

The implantation of a metal wire in the dorsum of mice is comparable to the surgical or orthopedic application of materials containing metals. Consistent with clinical observations that Ni has high irritancy,[1] only the Ni wire, among the metal wires implanted in this study, induced necrosis at 3 days in C57BL/6 mice (Fig. 1). Using rats implanted with a Ni wire, Wataha et al. found that Ni was ionized from the surface of the wire by body fluid and the concentration of Ni ions around the wire at 7 days was greater than 25 μg/g, resulting in necrosis.[9] Thus Ni ions are easily

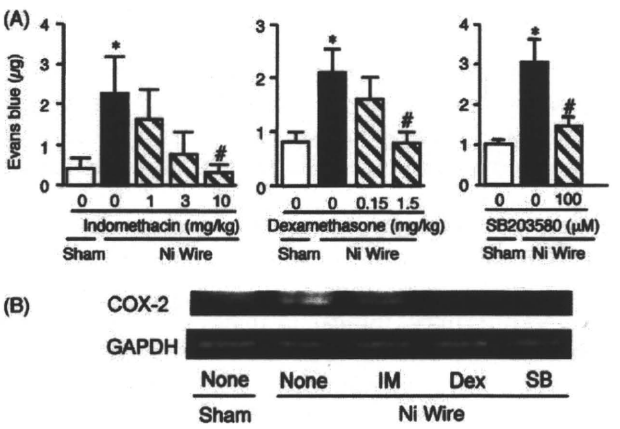

Figure 4. Effects of indomethacin, dexamethasone, and SB203580 on the vascular permeability and the expression of COX-2 mRNA induced by the implantation of a Ni wire Dexamethasone (0.15 and 1.5 mg/kg) or indomethacin (1, 3, and 10 mg/kg) was orally administered 3 or 1 h before the implantation of a Ni wire, respectively. SB203580 was injected into the site of implantation just after the implantation. (A) The exudation of Evans blue from 8 to 8.5 h after the implantation. Values are the means for five mice with the SEM shown by vertical bars. Statistical significance; $^{*}p < 0.05$ vs. the sham operation group and $^{\#}p < 0.05$ vs. the Ni wire implantation group. (B) The expression of the mRNA for COX-2 in the tissue surrounding the wire 4 h after the implantation. IM; indomethacin (10 mg/kg), Dex; dexamethasone (1.5 mg/kg), and SB; SB203580 (100 μM).